High JNK following Ras/Rpr/Tak1 over-expression in eye discs of *Drosophila* reduces post-pupariation ecdysone via Dilp8 causing early pupal death

Mukulika Ray and Subhash C. Lakhotia*

Cytogenetics Laboratory, Department of Zoology, Banaras Hindu University, India 221005

* Author for correspondence (Orcid no. 0000-0003-1842-8411)
Email: lakhotia@bhu.ac.in

Orcid ID:
Mukulika Ray: orcid.org/0000-0002-9064-818X
S. C. Lakhotia: orcid.org/0000-0003-1842-8411

Tele: +91-542-2368146

Running title: Dilp8 and early pupal death

One sentence Abstract

Elevated JNK activity following predominant over-expression of activated Ras or Reaper or Tak1 in *Drosophila* larval eye discs does not delay pupation but reduces post-pupariation ecdysone pulse via elevated Dilp8 and reduced Ptth, which results in early pupal death.

Abstract

We examined reasons for early pupal death following expression of certain transgenes with predominantly eye-disc specific *GMR-GAL4 or sev-GAL4* drivers in *Drosophila*. The *GMR-GAL4* or *sev-GAL4* driven expression of *UAS-Ras1*^{V12} transgene, producing activated Ras, resulted in early (~25-30Hr after pupa formation, APF) and late pupal death, respectively. Co-expression of *UAS-hsrω-RNAi* transgene or *EP3037* to down or up-regulate the hsrω lncRNAs with *sev-GAL4>UAS-Ras1*^{V12} advanced the death to 25-30Hr APF. The normal 8-12Hr APF ecdysone surge was absent in the early dying pupae. Exogenous ecdysone provided between 8-20Hr APF partially suppressed their early death. Microarray, qRT-PCR and immunostaining revealed substantial increase in some JNK pathway members in late larval eye discs, and of Dilp8 in eye discs, reduced transcripts of *ptth* in brain lobes and of ecdysone biosynthesis enzymes in prothoracic glands of 8-9Hr old pupae in genotypes that show early pupal death. We propose that the high JNK activity in eye discs of *GMR-GAL4>UAS-Ras1*^{V12} and *sev-GAL4>UAS-Ras1*^{V12} with altered hsrω transcript levels triggers greater Dilp8 secretion from them soon after pupa formation, which inhibits post-pupal ecdysone synthesis in prothoracic gland, leading to early pupal death. The early pupal death following *GMR-GAL4* driven expression of *UAS-rpr* or *UAS-tak1* was also associated with comparable enhanced JNK and Dilp8 signaling in eye discs. This study highlights how mis-regulated signaling in one tissue can have global deleterious consequences through downstream events in other tissues, reemphasizing role of inter organ signaling in life of an organism.

Keywords: *GMR-GAL4, sev-GAL4,* pMAPK, Halloween genes, lncRNA, *hsrω*

Introduction

An earlier study (*1*) indicated that *Ras* mutant alleles genetically interact with the *hsrω* long non-coding RNA (lncRNA) gene (*2*). With a view to explore this interaction further, we initiated studies using the GAL4-inducible activated form of DRas1 ($Ras1^{V12}$) (*3*) in conjunction with *hsrω-RNAi* transgene or an over-expressing *EP* allele of *hsrω* (*4*). We found that *GMR-GAL4* or *sev-GAL4* driven expression of activated Ras led to early and late pupal death, respectively. However, the *sev-GAL4* driven expression of activated Ras in background of increased or decreased hsrω nuclear transcripts further elevated Ras activity and concomitantly advanced the late pupal death to early stage (*5*). Several earlier studies have also reported pupal lethality when certain transgenes were expressed using the *GMR-GAL4* or *sev-GAL4* drivers (*4, 6*). Pupal lethality following expression of such transgenes under these two mostly eye-specific GAL4 drivers (*7-10*), has been intriguing since even a complete absence of eyes has no effect on viability of pupae and emergence of adult flies (*11*). Our recent finding (*12*) that, in addition to the well-known expression in eye disc cells, the *GMR-GAL4* and *sev-GAL4* drivers also express in several other cell types including specific neurons in the central nervous system (CNS), raised the possibility that the pupal death may be due to the transgene's ectopic expression in some of these other cells. We examine these possibilities in the present study.

Our study shows that the high JNK activity following ectopic over-expression of activated Ras in late larval eye discs is associated with elevated Dilp8 in early pupal eye discs, reduced *ptth* transcripts in early pupal brain lobes and reduction in transcripts of Halloween genes like *phantom* and *spok* in prothoracic gland. Together, these changes disrupt post-pupariation ecdysone synthesis and thereby cause early pupal death. Similar early pupal death and enhanced JNK and Dilp8 levels were observed in eye discs when *UAS-reaper* or *UAS-tak1* transgenes were ectopically expressed using the *GMR-GAL4* driver, reinforcing that it is the high JNK signaling in eye discs which leads to non-autonomous consequences, culminating in pupal death. Earlier reports (*13, 14*) have established that Dilp8, one of the eight insulin-like signal peptides in *Drosophila* (*15*), is secreted by damaged or inappropriately growing imaginal discs to delay metamorphosis by inhibiting ecdysone synthesis (*13, 14*). Our results show additional role of Dilp8 at pupal stages as well so that the post-pupariation enhanced Dilp8 activity can inhibit normal pupal development by lowering post-pupal ecdysone release, leading to pupal death. Present study also highlights the fact that changes in signaling cascade in one tissue (epithelia) can regulate downstream events in a tissue of completely different origin (brain and prothoracic gland).

Results

sev-GAL4 driven activated Ras expression causes late pupal lethality which is advanced by altered levels of hsrω transcripts

We used *sev-GAL4* driver to express the *UAS-*$Ras1^{V12}$ transgene which produces activated Ras and thus triggers the downstream signaling cascade without the need for ligand binding (*3*). As

reported earlier (*5*), the *sev-GAL4>UAS-Ras1^{V12}* pupae developed normally like wild type (Fig. 1A, E and I) till mid-pupal stages but a majority (~88%, N =1058) of them died subsequently (Fig. 1B, F and J); the remaining pupae eclosed with rough eyes due to the extra R7 photoreceptor. Interestingly, when levels of hsrω RNA were lowered by co-expression of *hsrω-RNAi* transgene (*4*) in *sev-GAL4>UAS-Ras1^{V12}* expressing pupae, development appeared normal till 8-9Hr after pupa formation (APF) (Fig. 1C, G and K) but further development was affected and ~ 96% (N =1177; (*5*)) of them died by 25-30Hr APF; the few survivors died as late pupae. Following co-expression of the *EP3037* over-expressing allele of *hsrω* (*4*) with *sev-GAL4>UAS-Ras1^{V12}*, 42% (N =1109; (*5*)) died as early pupae (~25-30Hr APF) and the rest as late pupae (Fig. 1D, H and L). Anterior part of all early dying pupae appeared empty with necrotic patch/es at the eye region becoming visible by 23-24Hr APF (Fig. 1K and L). Although they showed demarcation between head, thorax and abdomen, their Malpighian tubules, which become abdominal by this stage in *sev-GAL4>UAS-Ras1^{V12}* and in wild type (Fig. 2A), remained thoracic (Fig. 2B, C). Malpighian tubules in the early dying 23-24Hr old pupae also retained a comparatively longer anterior segment (Fig. 2E and F) like that seen in 14-15Hr old *sev-GAL4>UAS-Ras1^{V12}* pupae with their cells being far less compactly arranged than in 23-24Hr *sev-GAL4>UAS-Ras1^{V12}* pupae (Fig. 2G-I). Interestingly, the salivary glands, which normally disappear by this stage of pupal development, also persisted in pupae co-expressing *sev-GAL4>UAS-Ras1^{V12}* and *hsrω-RNAi* or *EP3037* beyond the 15-16Hr APF stage (Fig. 2J-L). The other early pupal phenotype persisting in the early dying pupae was the *sev-GAL4* driven *UAS-GFP* expression in the 7 pairs of dorso-medially placed neurons in each of the posterior neuromeres in abdominal ganglia (*12*). In *sev-GAL4>UAS-Ras1^{V12}* pupae (Fig. 2M), like that in wild type, all the 7 pairs of these dorso-medial neurons showed *UAS-GFP* expression at 8-9Hr APF. As reported earlier (*12*), the GFP expression in all of these, except the anterior-most pair, disappeared in 23-24Hr old wild type and *sev-GAL4>UAS-Ras1^{V12}* pupae (Fig. 2P). However, all the 7 pairs of these neurons continued to show *UAS-GFP* expression in 23-24Hr old *sev-GAL4>UAS-Ras1^{V12} hsrω-RNAi* or *sev-GAL4>UAS-Ras1^{V12} EP3037* pupae (Fig. 2Q, R). The small proportion of pupae that survive beyond 23-24Hr APF showed normal developmental changes as in wild type or *sev-GAL4>UAS-Ras1^{V12}* pupae of comparable age. However, their later development was affected and they died as late pupae.

GMR-GAL4 driven activated Ras expression causes early pupal lethality irrespective of hsrω transcript levels

Unlike the *sev-GAL4* expression in a few photoreceptor cells in each ommatidium of eye discs, the *GMR-GAL4* expression is seen in nearly all cells of the eye disc behind the morphogenetic furrow (*12*). The *sev-GAL4* driven expression of *UAS-Ras1^{V12}* resulted in late pupal lethality and that with the *GMR-GAL4* driver resulted in 100% early pupal lethality with developmental defects setting in by 8-9Hr APF stage. Unlike the 13-14 or 19-20Hr old wild type pupae (Fig. 1M, Q), those expressing *GMR-GAL4>UAS-Ras1^{V12}* did not show demarcation of head, thorax and abdominal regions (Fig. 1N and R). A necrotic patch appeared by 19-20Hr APF at each of prospective adult eye site (Fig. 1R). The early disappearing dorso-medial pairs of neurons in the

abdominal ganglia also continued to show GFP expression till 20-24Hr APF in the dying *GMR-GAL4>UAS-Ras1^{V12}* pupae (see Fig. 3I-L). Co-expression of *EP3037* or *hsrω-RNAi* with *GMR-GAL4>UAS-Ras1^{V12}* did not affect the time of pupal death as all of them died at the early stage with similar phenotypes (Fig. 1N-P, R-T).

Ecdysone signaling at early pupal stages compromised in the early dying pupae

The above phenotypes indicated that the pupae that die around 25-30Hr APF fail to undergo the early pupal changes that follow the ecdysone pulse beginning at 8-10Hr APF (*16*). Therefore, we examined the distribution of Broad, one of the early ecdysone signaling responders (*17, 18*), in late third instar larval and pupal (12-13 and 24-25Hr APF stage) ventral ganglia of different genotypes with a Broad-core antibody (*19*). In all the genotypes intense and uniform nuclear fluorescence with little cytoplasmic signal (Fig. 3A-D) was seen in Broad positive ventral ganglia cells from early pupal stages (12-13Hr APF). However, beginning at 16Hr APF, the distribution of Broad in *sev-GAL4>UAS-GFP* and *sev-GAL4>UAS-Ras1^{V12}* ventral ganglia changed from a uniform nuclear distribution seen in younger pupae, to a few intense peri-nuclear granules (Fig. 3E and F); its presence in cytoplasm was also stronger than in earlier stages. Interestingly, ventral ganglia in pupae co-expressing *hsrω-RNAi* or *EP3037* with *Ras1^{V12}* under the *sev-GAL4* driver did not show these changes since even at 24-25Hr APF, most Broad positive cells showed more or less uniform pan-nuclear distribution of Broad with low presence in cytoplasm (Fig. 3G, H). A few nuclei in the 24-25Hr old pupal ventral ganglia co-expressing *sev-GAL4* driven *Ras1^{V12}* and *hsrω-RNAi* or *EP3037* showed Broad in a punctate or granular form, but these puncta were distributed across the nuclear area rather than being typically peri-nuclear as in the same age *sev-GAL4>UAS-GFP* and *sev-GAL4>UAS-Ras1^{V12}* pupal ventral ganglia (Fig. 3).

The *GMR-GAL4>UAS-GFP* expressing ventral ganglia from 16-17 and 20-21Hr old pupae (Fig. 3I, K) showed the Broad protein as in corresponding age *sev-GAL4>UAS-GFP* and *sev-GAL4>UAS-Ras1^{V12}* pupae. However, the Broad protein retained its uniformly strong pan-nuclear distribution in most of the Broad positive cells in *>UAS-Ras1^{V12}* ventral ganglia from 20-21Hr old pupae (Fig. 3J) as in the 12-13Hr APF or younger pupae; the cytoplasmic presence of Broad was also low in these cells. The *GMR-GAL4* driven co-expression of *hsrω-RNAi* or *EP3037* with *UAS-Ras1^{V12}* did not alter the Broad distribution (Fig. 3K, L).

Interestingly, none of the *sev-GAL4>UAS-GFP* or *GMR-GAL4>UAS-GFP* expressing neurons in the ventral ganglia (marked by white arrows in Fig 2E-H), showed Broad expression, neither at 8-9Hr nor at 24-25Hr APF stage (Fig. 3) in any of the genotypes.

The post-pupation ecdysone levels reduced in early dying pupae

The absence of redistribution of Broad protein in 16Hr or older pupae that would die at about 25-30Hr APF further indicated a failure of the post-pupation ecdysone signaling. Immunoassay for 20-hydroxy-ecdysone indeed revealed that while ecdysone levels in 8-9Hr old pupae expressing

sev-GAL4 driven activated Ras alone or together with *hsrω-RNAi* transgene or *EP3037* allele were comparable to those in similar age *sev-GAL4>UAS-GFP* pupae (Fig. 4A), the 24-25Hr APF stage pupae co-expressing *hsrω-RNAi* or *EP3037* with $Ras1^{V12}$ under the *sev-GAL4* driver did not display the increase in ecdysone levels that is characteristically seen (*16*) in those expressing the *sev-GAL4* driven *UAS-GFP* or only activated Ras or only the *hsrω-RNAi* transgene or *EP3037* (Fig. 4A). The ecdysone levels in 24-25Hr APF stage pupae expressing activated Ras under the *GMR-GAL4* driver were also significantly lower than in the corresponding age *GMR-GAL4>UAS-GFP* control pupae (Fig 4B).

Further support for reduced levels of ecdysone being responsible for the early pupal death was obtained by examining phenotypes of otherwise wild type early pupae in which the ecdysone levels were conditionally reduced using the temperature sensitive ecd^{1} allele (*20*). This temperature-sensitive mutation inhibits production of ecdysone when grown at the restrictive temperature (29-30°C). The *sev-GAL4>UAS-GFP;* ecd^{1} larvae were reared at 24°C and 0-1Hr old white prepupae were transferred to 30°C to conditionally inhibit further ecdysone synthesis. About 50% of these pupae showed early death by 25-30Hr APF while the remaining ones died as late pupae (Table 1). The dying 24-25Hr old *sev-GAL4>UAS-GFP;* ecd^{1} pupae, reared since beginning of pupation at 30°C, showed persistence of the dorso-medial pairs of segmental neurons in ventral ganglia, less compact arrangement of Malpighian tubule cells (Supplementary Fig. S1 A, B) and the other developmental defects seen in pupae co-expressing *sev-GAL4* driven activated Ras and *hsrω-RNAi* or *EP3037*.

Externally provided ecdysone partially rescues the early pupal death

To further confirm that the early pupal death following *sev-GAL4* driven co-expression of $Ras1^{V12}$ and *hsrω-RNAi* or *EP3037* was due to sub-threshold levels of ecdysone, we exposed 8-9Hr old pupae of different genotypes to exogenous ecdysone by incubating them in 1 µg/ml 20-hydroxyecdysone solution for 12Hr, following which they were taken out and allowed to develop further. To confirm effectiveness of such exogenous exposure to ecdysone, we used ecd^{1} mutant pupae as control. Fresh 0-1Hr old *sev-GAL4>UAS-GFP;* ecd^{1} white prepupae, grown through the larval period at 24°C, were transferred to 30°C to block further ecdysone synthesis. After 8Hr at 30°C, they were transferred to the 20-hydroxy-ecdysone solution for 12Hr at 30°C so that while the endogenous ecdysone synthesis remained inhibited, it was available from the incubation medium. After the 12Hr ecdysone exposure, the pupae were returned to 30°C for further development. As noted above and from the data in Table 1, about 50% *sev-GAL4>UAS-GFP;* ecd^{1} pupae maintained at 30°C from 0-1Hr pre-pupa stage onwards without any exogenous ecdysone died by 25-30Hr APF. However, there was a 2-fold decrease in the early death of ecd^{1} pupae maintained at 30°C but exposed to exogenous ecdysone from 8 to 20Hr APF (Table 1), although none of them eclosed as flies. Significantly, the pre-pupal to pupal metamorphic changes in these surviving pupae occurred normally so that the dorso-medial pairs of segmental neurons in ventral ganglia and Malpighian tubules displayed the expected changes (Supplementary Fig. S1 C, D). The survival of a significant proportion of ecd^{1} pupae, maintained

at 30°C while being exposed to exogenous ecdysone, clearly indicated that the moulting hormone penetrated the early pupal case in at least some of them and rescued the absence of endogenous ecdysone in *ecd*^{1} pupae at the restrictive temperature. The failure of all the exogenous ecdysone exposed pupae to survive beyond the early stage may be due to a variable penetration of ecdysone and other biological variables.

When 8-9Hr old pupae co-expressing *sev-GAL4* driven activated Ras and *hsrω-RNAi* or activated Ras and *EP3037* were exposed to exogenous 20-hydroxy-ecdysone as above, there was a near 2-fold increase in those continuing to develop to late stages, although none of them emerged as flies (Table 1). The somewhat lesser increase (1.4 fold, Table 1) in survival of the ecdysone exposed *sev-GAL4>UAS-Ras1*^{V12} *hsrω-RNAi* pupae beyond the early stage seems to be related to the fact that a larger proportion of them die early (see above, Fig. 1). Together, these results confirm that *sev-GAL4* driven activated Ras and *hsrω-RNAi* or activated Ras and *EP3037* or *GMR-GAL4* driven activated Ras expression alone, somehow inhibited ecdysone release that occurs after 8-9Hr pupal stage and therefore, such pupae fail to undergo the expected metamorphic changes.

Early dying pupae with lowered *ptth* and Halloween genes and elevated expression of *dilp8* and some JNK pathway genes

Since the *GMR-GAL4* and *sev-GAL4* drivers do not express in prothoracic glands (*12*), a reduction in ecdysone levels in early pupae was unexpected. Therefore, to identify the signals that may affect ecdysone levels following co-expression of *sev-GAL4* driven *Ras1*^{V12} and *hsrω*-RNAi or *EP3037*, total RNAs from 16-17Hr old pupae of different genotypes (*sev-GAL4>UAS-GFP, sev-GAL4>UAS-Ras1*^{V12}, *sev-GAL4>UAS-Ras1*^{V12} *hsrω-RNAi* and *sev-GAL4>UAS-Ras1*^{V12} *EP3037*) were used for a microarray based transcriptome analysis. A pair wise comparison between different genotypes revealed significant up- or down-regulation of many genes belonging to diverse GO categories (see Supplementary Table S1). In order to narrow down on the genes which may be causally associated with the early pupal death, we focused on those that were commonly up- or down-regulated in *sev-GAL4>UAS-Ras1*^{V12} *hsrω-RNAi* and *sev-GAL4>UAS-Ras1*^{V12} *EP3037* samples when compared with their levels in *sev-GAL4>UAS-Ras1*^{V12} (columns 1 and 2 in Supplementary Table S1). The commonly up-regulated groups of genes in *sev-GAL4>UAS-Ras1*^{V12} *hsrω-RNAi* and *sev-GAL4>UAS-Ras1*^{V12} *EP3037* larvae included, among many others, those associated with stress responses, cell and tissue death pathways, autophagy, toll signaling, innate immune system etc. Some of these seem to be primarily due to activated Ras or altered *hsrω* expression since the Ras/MAPK pathway is known to regulate immune response (*21, 22*) while the hsrω transcripts have roles in stress responses, cell death and several other pathways (*2, 23, 24*). More interestingly, several genes involved in lipid and steroid biosynthesis processes were commonly down-regulated in both the early pupal death associated genotypes (*sev-GAL4>UAS-Ras1*^{V12} *hsrω-RNAi* and *sev-GAL4>UAS-Ras1*^{V12} *EP3037*) (Supplementary Table S1), which appears to be in agreement with the above noted reduced levels of ecdysone in the early dying pupae.

Since damage to or tumorous growth of imaginal discs is reported (*13, 14*) to affect ecdysone synthesis through up regulation of Dilp8 levels and JNK signaling, we examined the microarray data for levels of transcripts of genes involved in ecdysone biosynthesis and insulin- and JNK-signaling pathways through pair wise comparisons of different genotypes (Table 2), taking >1.5 fold difference as significant. Three (*spookier, phantom* and *shadow*) of the five 20-hydroxy-ecdysone synthesis related Halloween genes (*25*) showed consistent down-regulation in *sev-GAL4>UAS-Ras1^{V12} hsrω-RNAi* and *sev-GAL4>UAS-Ras1^{V12} EP3037* genotypes when compared with *sev-GAL4>UAS-Ras1^{V12}* pupae, while *shade* did not show any significant change and *disembodied* displayed up-regulation. The down-regulation of spookier, phantom and shadow transcripts in 16-17Hr old *sev-GAL4>UAS-Ras1^{V12} hsrω-RNAi* and *sev-GAL4>UAS-Ras1^{V12} EP3037* pupae correlates with the above noted (Fig. 4) reduced ecdysone levels since while the *spookier* and *phantom* genes act at early stages in ecdysone biosynthesis (*25*), the *shadow* gene product converts 2-deoxyecdysone into ecdysone (*26*).

Of the eight known Dilps (Dilp1-8) in *Drosophila* (*15*), only the levels of Dilp8 were significantly up-regulated in *sev-GAL4>UAS-Ras1^{V12} hsrω-RNAi* and *sev-GAL4>UAS-Ras1^{V12} EP3037* genotypes when compared with *sev-GAL4>UAS-GFP* or *sev-GAL4>UAS-Ras1^{V12}* (Table 2). Interestingly, when compared with *sev-GAL4>UAS-Ras1^{V12}*, the increase in Dilp8 transcripts in *sev-GAL4>UAS-Ras1^{V12} hsrω-RNAi* was about 2 fold greater than that in *sev-GAL4>UAS-Ras1^{V12} EP3037* (Table 1). This difference correlates with the much higher frequency of death of former as early pupae than of *sev-GAL4>UAS-Ras1^{V12} EP3037*.

Like the Dilp8, transcripts of *tobi* (*target of brain insulin*) were also significantly up-regulated (Table 2) when *sev-GAL4>UAS-Ras1^{V12}* was expressed in conjunction with *hsrω-RNAi* or *EP3037*. It has recently (*27, 28*) been shown that the Dilp8 action on ecdysone synthesis in prothoracic gland may involve the neuronal relaxin receptor Lgr3. Our microarray data indicated that the *lgr3* transcripts were only marginally elevated in *sev-GAL4>UAS-Ras1^{V12} hsrω-RNAi* expressing early pupae but not significantly affected in *sev-GAL4>UAS-Ras1^{V12} EP3037* individuals.

Analysis of the microarray data for total RNA from 16-17Hr old pupae revealed considerable variability in levels of different members of the JNK-signaling pathway in different genotypes (Table 2). Interestingly, a greater number of the JNK pathway genes were up-regulated in *sev-GAL4>UAS-Ras1^{V12} hsrω-RNAi* when compared with *sev-GAL4>UAS-GFP* or *sev-GAL4>UAS-Ras1^{V12}* genotypes. On the other hand, several of the JNK pathway genes appeared down-regulated in *sev-GAL4>UAS-Ras1^{V12} EP3037* genotypes when compared with *sev-GAL4>UAS-GFP* or *sev-GAL4>UAS-Ras1^{V12}* genotypes (Table 2). However, genes like *eiger*, *gadd45* and *takl1* were significantly up-regulated in *sev-GAL4>UAS-Ras1^{V12} hsrω-RNAi* as well as in *sev-GAL4>UAS-Ras1^{V12} EP3037* genotypes, while *tak1* was down-regulated in both. It is noteworthy that the fold change for each of these genes was greater in case of *sev-GAL4>UAS-Ras1^{V12} hsrω-RNAi* than in *sev-GAL4>UAS-Ras1^{V12}* EP3037.

We validated some of the microarray data by qRT-PCR with RNA samples from late larval and early pupal (8-9Hr APF) eye discs and/or prothoracic glands (Fig. 5A). In agreement with the microarray data for whole pupal RNA, qRT-PCR of 8-9Hr old pupal eye disc RNA confirmed significant up-regulation of transcripts of the JNK signaling pathway genes like *tak1-like 1, eiger 2, gadd45* and *puckered* in *sev-GAL4>UAS-Ras1^{V12} hsrω-RNAi* and *sev-GAL4>UAS-Ras1^{V12} EP3037* when compared with same age *sev-GAL4>UAS-Ras1^{V12}* eye discs (Fig. 5A). Interestingly the late third instar larval eye discs did not show much difference in levels of these transcripts between the different genotypes (Fig. 5A).

Quantification of *dilp8* transcripts from late third instar larval and 8-9Hr pupal eye discs of different genotypes by qRT-PCR revealed that, in agreement with microarray data for total pupal RNA, *dilp8* transcripts were greatly (65-120 folds) elevated in *sev-GAL4>UAS-Ras1^{V12} hsrω-RNAi* and *sev-GAL4>UAS-Ras1^{V12} EP3037* pupal eye discs when compared with those expressing only the activated Ras (Fig. 5A). On the other hand, levels of *dilp8* transcripts in late third instar larval eye discs showed only a marginal up-regulation in *sev-GAL4>UAS-Ras1^{V12} hsrω-RNAi* and *sev-GAL4>UAS-Ras1^{V12} EP3037* eye discs (Fig. 5A). Compared to control, the brain lobes and ventral ganglia of early dying pupae also showed substantial increase in *dilp8* transcripts, more so in brain lobes of *sev-GAL4>UAS-Ras1^{V12} hsrω-RNAi* (Fig. 5B).

Down-regulation of *spookier* and *phantom* transcripts in *sev-GAL4>UAS-Ras1^{V12} hsrω-RNAi* and *sev-GAL4>UAS-Ras1^{V12} EP3037* genotypes at early pupal stage was also validated by qRT-PCR using RNA from 8-9Hr old pupal prothoracic glands. Compared to *sev-GAL4>UAS-Ras1^{V12}*, both transcripts showed greater reduction in *sev-GAL4>UAS-Ras1^{V12} hsrω-RNAi* and *sev-GAL4>UAS-Ras1^{V12} EP3037* pupal (Fig 5A) than in larval prothoracic glands. Intriguingly, *sev-GAL4>UAS-Ras1^{V12} hsrω-RNAi* larval eye discs showed up-regulation of *spookier* and *phantom* transcripts (Fig. 5A).

Since Dilp8 is reported to inhibit ecdysone synthesis triggering signals from the brain (*13, 14*), we examined levels of *ptth* transcripts in brain in the early dying pupae. We also checked the transcripts of Dilp8 receptor in brain (*28, 29*). As expected, the *ptth* transcripts were less abundant in larval brain lobes of early dying individuals, and this was further reduced in early pupae so much so that no transcripts were detected in pupal brain lobes of *sev-GAL4>UAS-Ras1^{V12} hsrω-RNAi* (Fig 5B). On the other hand, transcripts of none of the three Dilp8 receptors, viz., *lgr3*, *inr* and *drl*, showed any substantial reduction in early pupal brain lobes or ventral ganglia. Surprisingly, the *inr* transcript levels in *sev-GAL4>UAS-Ras1^{V12} EP3037* showed about 4 fold up-regulation when compared with *sev-GAL4>UAS-Ras1^{V12}* (Fig 5B). Since there was no change in *dilp8* transcripts in eye discs of third instar larvae, levels of the Dilp8 receptor transcripts were not examined in larval brain lobes.

The *gadd45* transcripts in pupal brain lobes as well as ventral ganglia showed only a two fold increase (Fig 5B).

Dilp8 protein levels elevated in early pupal but not larval eye discs or in larval and pupal CNS in early dying genotypes

Elevation in Dilp8 in the early dying pupae, but not in late third instar eye discs was confirmed by immunostaining of eye discs with a antibody recognizing Dilp8 (*14*). A faint presence of Dilp8 was seen in the cytoplasm of peripodial cells of late third instar larval eye discs of all the genotypes (Fig. 6A-D). The peripodial cells of 8-9 Hr pupal eye discs (Fig. 6E-H) co-expressing *sev-GAL4>UAS-Ras1^{V12}* and *hsrω-RNAi* and *sev-GAL4>UAS-Ras1^{V12} EP3037* showed stronger Dilp8 staining (Fig. 6G, H) than in *sev-GAL4>UAS-GFP* (Fig. 6E) or *sev-GAL4>UAS-Ras1^{V12}* (Fig. 6F) pupal eye discs (for quantification of immunostaining, see Supplementary Fig. S2).

Since the *sevGAL4* and *GMR-GAL4* drivers also express in certain neurons in brain lobes and ventral ganglia (*12*), we immunostained early pupal CNS of 8-9Hr old pupae in *sevGL4>UAS-GFP*, *sev-GAL4>UAS-Ras1^{V12}*, *sev-GAL4>UAS-Ras1^{V12} hsrω-RNAi* and *sev-GAL4>UAS-Ras1^{V12} EP3037* (Fig. 7A-H) with Dilp8 ab. A low abundance of Dilp8 was seen all through the brain and ventral ganglia of *sevGL4>UAS-GFP* (Fig. 7A, E, I). It is very interesting that none of the *sevGAL4>UAS-GFP* expressing neurons in brain and ventral ganglia (*12*) of *sev-GAL4>UAS-Ras1^{V12}*, and thus also expressing the *Ras^{V12}* transgene, showed elevation in Dilp8 expression beyond the low expression seen in adjoining cells (Fig. 7B, F, J). Likewise, the Dilp8 expression in the 8-9Hr old pupal *sev-GAL4>UAS-Ras1^{V12} hsrω-RNAi* and *sev-GAL4>UAS-Ras1^{V12} EP3037* brain lobes and ventral ganglia remained similar to that in *sevGAL4>UAS-GFP* and *sev-GAL4>UAS-Ras1^{V12}* (Fig. 7A-L). Intriguingly, a group of 4 neurons located in mid-lateral part in each of the brain-hemispheres in all the four genotypes showed strong Dilp8 presence in cytoplasm and their axonal projections, which followed a semi-circular path to reach the prothoracic gland initiation region (Fig. 7E-H). The proximal part of prothoracic gland also showed intense Dilp8 staining. It is, however, to be noted that, unlike the above noted increase in levels of *dilp8* transcripts in early pupal CNS of *sev-GAL4>UAS-Ras1^{V12} hsrω-RNAi* and *sev-GAL4>UAS-Ras1^{V12} EP3037*, the levels of Dilp8 protein staining in CNS, including these specific 4 pairs of neurons and the basal part of the prothoracic gland, remained comparable in all the genotypes. This indicates that despite the increase in transcript levels, the *sevGAL4* driven expression of activated Ras without or with concurrent altered *hsrω* expression did not affect Dilp8 protein levels in the CNS.

Phosphorylated JNK elevated in larval eye discs but not in CNS in early dying genotypes

Immunostaining for phosphorylated JNK (p-JNK, Basket) in *sev-GAL4>UAS-GFP* late third instar eye discs revealed low cytoplasmic p-JNK in photoreceptor cells (Fig. 8A). Photoreceptor cells from *sev-GAL4>UAS-Ras1^{V12}* larval discs showed slightly elevated p-JNK staining (Fig. 8B). Interestingly, co-expression of *hsrω-RNAi* transgene with *sev-GAL4>UAS-Ras1^{V12}* resulted in a much greater increase in p-JNK (Fig. 8C). Up-regulation of hsrω transcripts in *sev-GAL4>UAS-Ras1^{V12}* expressing larval eye discs was also associated with increase in p-JNK levels when compared with *sev-GAL4>UAS-GFP* (Fig. 8D), although the increase was less than that in *sev-GAL4>UAS-Ras1^{V12} hsrω-RNAi* eye discs. Immunostaining for p-JNK in 8-9Hr pupal discs also showed increase in *sev-GAL4>UAS-Ras1^{V12} hsrω-RNAi* and in *sev-GAL4>UAS-Ras1^{V12} EP3037* compared to *sev-GAL4>UAS-Ras1^{V12}* (Supplementary Fig. S3A-C).

Immunostaining of 8-9 Hr old pupal brain ganglia for p-JNK revealed that its expression was not affected by *sevGAL4>UAS-Ras*^{V12} expression, without or with concurrent altered *hsrω* levels. Brain lobes showed comparable JNK staining in all the genotypes with a stronger expression in the Mushroom body (Fig. 8E-H).

We did not examine the p-JNK immunostaining in late larval CNS since we found that the levels of p-MAPK, which is required for activation of JNK (*30*), in CNS were not significantly affected in any of these genotypes, except for a marginal increase in the nuclear p-MAPK in the *UAS-GFP* expressing medio-dorsal pairs of neurons in abdominal ganglia of *sevGAL4>UAS-Ras*^{V12} *UAS-hsrω-RNAi* and *sevGAL4>UAS-Ras*^{V12} *EP3037*larvae (Supplementary Fig. S3 D-I).

We have recently reported (*5*) that *sev-GAL4* driven co-expression of *Ras1*^{V12} with *hsrω-RNAi* or *EP3037* substantially enhances levels of activated Ras in eye discs. To ascertain if the above noted elevated p-JNK levels in eye discs co-expressing *sev-GAL4* driven *Ras1*^{V12} with *hsrω-RNAi* or *EP3037* was indeed dependent upon the high activated Ras expression, we co-expressed *UAS-RafRBDFLAG* in these genotypes. The RafRBDFLAG construct acts as a dominant negative suppressor of Ras signaling (*31*). We examined effect of *sev-GAL4* driven co-expression of *RafRBDFLAG* with *Ras1*^{V12} without or with *hsrω-RNAi* or *EP3037* expression on pupal survival and p-JNK levels in eye discs of late 3rd instar larvae. Interestingly, there was no pupal lethality when *RafRBDFLAG* was co-expressed with *sev-GAL4* driven *Ras1*^{V12} without or with *hsrω-RNAi* or *EP3037* expression (see Table 3). Concomitantly, the p-JNK levels were also not elevated in any of the genotypes when compared with those in *sev-GAL4>UAS-GFP/UAS-RafRBDFLAG* eye discs (Fig. 8I-L). Data on the relative quantities of p-JNK (Fig. 9A) in photoreceptor cells of different genotypes, obtained using the Histo tool of the LSM510 Meta software on projection images of 12 optical sections through the photoreceptor arrays in each disc, confirmed the significant increase in p-JNK in *sev-GAL4>UAS-Ras1*^{V12} *hsrω-RNAi* and *sev-GAL4>UAS-Ras1*^{V12} *EP3037* eye discs but not when *RafRBDFLAG* was also co-expressed.

These findings establish that the observed increase in p-JNK levels in *sevGAL4>UAS-Ras*^{V12} *UAS-hsrω-RNAi* and *sevGAL4>UAS-Ras*^{V12} *EP3037* late larval eye discs is indeed related to the very high levels of activated Ras in them (*5*).

GMR-GAL4 driven expression of other transgenes causing early pupal death also show enhanced JNK and Dilp8 activity in eye discs

With a view to examine if the JNK and Dilp8 signaling was elevated in other cases also where the *GMR-GAL4* driven expression of a transgene results in early pupal lethality, we examined effects of *GMR-GAL4* driven expression of *UAS-GFP* or *UAS-127Q* or *UAS-Ras1*^{V12} or *UAS-rpr* or *UAS-tak1* on pupal lethality and p-JNK levels in their larval eye discs. *GMR-GAL4* driven expression of *UAS-GFP* or *UAS-127Q* does not cause any pupal lethality (above results and (*4*) while that of *UAS-Ras1*^{V12} (above results) or *UAS–rpr* (Table 3, also see (*6*) or *UAS-tak1* (present observations, Table 3) cause early pupal death in a manner similar to that noted above for *GMR-GAL4>UAS-Ras1*^{V12} or *sev-GAL4>UAS-Ras1*^{V12} with co-expression of *UAS-hsrω-RNAi* or

EP3037. Immunostaining for p-JNK in late larval eye discs of these different genotypes revealed that while those from *GMR-GAL4* driven GFP or 127Q (Fig. 9D and E) larvae showed the normal low to moderate p-JNK presence in eye discs, those expressing *GMR-GAL4* driven *UAS-Ras1^{V12}* or *UAS–rpr* or *UAS-tak1* displayed very high p-JNK staining (Fig. 9F-H). Tak1 is a known up-regulator of JNK signaling (*32, 33*), and accordingly eye discs expressing this transgene showed a widespread p-JNK staining (Fig. 9G). Thus, all the examined genotypes that showed early pupal death also showed high p-JNK in late larval eye discs.

To further confirm enhanced JNK signaling and consequent Dilp8 activity, we examined levels of transcripts of *gadd45*, one of the JNK pathway genes and *dilp8*, in late larval and early pupal *GMR-GAL4>UAS-GFP*, *GMR-GAL4>UAS-Ras^{V12}*, *GMR-GAL4>UAS-tak^{1}* and *GMR-GAL4>UAS-127Q* eye discs. In agreement with the absence of pupal death in case of *GMR-GAL4>UAS-127Q*, neither *dilp8* nor *gadd45* transcripts showed any appreciable changes in eye discs when compared to the controls (*GMR-GAL4>UAS-GFP*). In the cases of early dying *GMR-GAL4>UAS-Ras^{V12}* and *GMR-GAL4>UAS-tak^{1}* individuals, *dilp8* transcripts were more abundant at pupal than at larval stages compared to control (Fig. 9C) In the case of *GMR-GAL4>UAS-tak^{1}* even larval eye discs showed about 3 fold increase in *dilp8* transcripts than corresponding *GMR-GAL4>UAS-GFP* eye discs. The increase in their early pupal eye discs was more than 6 fold. Since Tak^{1} is a JNKKK (*34, 35*), the observed increase in *dilp8* transcripts in *GMR-GAL4>UAS-tak^{1}* eye discs agrees with a role of JNK signaling in Dlip8 expression. The *gadd45* transcripts also showed significant increase in *GMR-GAL4>UAS-tak^{1}* early pupal eye discs compared to controls.

The pupal survival, p-JNK and Dilp8 staining patterns in the different genotypes examined in our study are summarized in Table 3. This comparison shows that both the JNK and Dilp8 signaling cascades were up-regulated in larval and early pupal eye discs, respectively, in all the genotypes that displayed high death at about 23-25Hr APF.

Discussion

Present study examines possible reasons for the unexpected pupal death following the predominantly eye disc specific *GMR-GAL4* or *sev-GAL4* driven expression of certain transgenes. We found that the early dying pupae do not show the early metamorphic changes and this correlated with absence of the ecdysone surge that normally occurs beyond the 8-12Hr APF (*16*). In agreement with our hypothesis that this decrease in ecdysone level leads to early pupal death, we found that conditional inhibition of ecdysone synthesis during early pupal stage in the temperature sensitive *ecd^{1}* mutant also results in early pupal death like that in the other genotypes examined by us, and that this can be significantly suppressed by exogenous ecdysone provided during 8 to 20Hr APF.

In agreement with the reduced levels of ecdysone in pupae, our microarray and qRT-PCR data showed that key genes like *spookier* and *phantom*, involved in the early ecdysone biosynthesis steps, are indeed down-regulated in early pupal prothoracic glands in genotypes that show early

pupal death but not at late third instar stage. Together, our findings clearly indicate that the reduced ecdysone titer after the 8-12Hr APF stage in these genotypes is responsible for the early pupal death. The observed unaltered levels of the *shade* gene transcripts, which encode Cyp314a1 that adds a hydroxyl group to ecdysone in the final step, may not be relevant in present context since its substrate, ecdysone, would be limiting due to down-regulated spookier, phantom and shadow transcripts in *sev-GAL4>UAS-Ras1^{V12} hsrω-RNAi* and *sev-GAL4>UAS-Ras1^{V12} EP3037* genotypes. Moreover, the *shade* gene product converts ecdysone to 20-hydroxy-ecdysone in fat bodies (*25*). The observed elevation in levels of disembodied transcripts (Table 2) in the total pupal RNA may appear incongruent, since the Disembodied protein acts between Spookier and Phantom in ecdysone synthesis and, therefore, was expected to be down-regulated like *spookier* and *phantom*. However, it is to be noted that the microarray data is derived from total pupal RNA rather than from only the prothoracic glands. Further, since *disemodied* can be regulated independent of *spookier* (*36*), it may express in some other tissues as well.

Since the ecdysone synthesis and release from prothoracic gland is regulated by neuro-endocrine signals emanating from the CNS (*37, 38*), it is possible that the ectopic expression of the *sev-GAL4* and *GMR-GAL4* drivers in certain neurons in brain and ventral ganglia (*12*) may directly affect ecdysone synthesis. However, our results that the *sev-GAL4* and *GMR-GAL4* expressing CNS neurons persist when ecdysone synthesis in prothoracic glands was conditionally inhibited using the temperature sensitive *ecd^{1}* mutant allele (*20, 39*) and disappeared in individuals escaping early death by exogenous ecdysone indicate that persistence of GFP expression in these CNS neurons in the early dying pupae is a consequence, rather than a cause, of the reduced ecdysone signaling.

Further support for the primary role of eye discs in the early pupal death in *sev-GAL4>UAS-Ras1^{V12} hsrω-RNAi* or *sev-GAL4>UAS-Ras1^{V12} EP3037* genotypes is provided by the fact that unlike the almost comparable expression of the *GMR-GAL4* and *sev-GAL4* drivers in brain and abdominal ganglia (*12*), that in the eye discs is significantly different. While the *sev-GAL4* driver expresses only in a subset of photoreceptor cells, the *GMR-GAL4* is expressed more extensively in nearly all cells posterior to the morphogenetic furrow (*7-10, 12*). Ectopic expression of activated Ras disrupts development of eye discs (*3*) and as known (*3, 7, 10*), we also found more severe effects on eye development following *GMR-GAL4>UAS-Ras1^{V12}* expression. We have also seen that unlike in discs expressing only *sev-GAL4>UAS-Ras1^{V12}*, co-expression of *sev-GAL4>UAS-Ras1^{V12}* with *hsrω-RNAi* or *EP3037* results in enhanced Ras expression which spreads non-autonomously to neighbouring cells to a much greater extent (*5*). Consequently, the cumulative effect of activated Ras expression in these genotypes may become nearly as strong as that in *GMR-GAL4>UAS-Ras1^{V12}* eye discs. Furthermore, we found that the CNS in genotypes displaying early pupal death did not show enhanced p-MAPK or JNK activity. Taken together, the more severe damage in eye discs in all these conditions correlates with the early pupal death. Therefore, we believe that the early pupal death following *GMR-GAL4>UAS-Ras1^{V12}*or *GMR-GAL4>UAS-rpr* or *GMR-GAL4>UAS-tak1* expression or following co-expression of

sevGAL4>UAS-Ras1^{V12} and *hsrω-RNAi* or *EP3037* is most likely related to the signals primarily emanating from eye discs rather than the CNS.

The signal peptide Dilp8 plays a significant role in coordinating imaginal tissue growth and ecdysone synthesis in prothoracic gland (*13, 14, 40, 41*). Damaged or abnormally growing discs are believed to secrete Dilp8 to transiently delay ecdysone synthesis (*13, 42*). The enhanced levels of Dilp8 transcripts in early pupal eye discs and Dilp8 protein in their peripodial cells in all the genotypes that exhibited early pupal death confirm that the disrupted eye disc development following *GMR-GAL4>UAS-Ras1*^{V12} expression or *sev-GAL4>UAS-Ras1*^{V12} expression in background of altered hsrω transcripts trigger the pupal discs to activate Dilp8 synthesis and its secretion via the peripodial cells.

A recent study (*29*) has not reported any lethality at larval or pupal stages following global over-expression of Dilp8 using the ubiquitously expressed *tubulin* promoter. These results may appear in conflict with our finding that elevated Dilp8 levels in eye discs correlate with early pupal death. However, it is possible that the *tubulin* promoter may not have enhanced Dilp8 to the threshold level required to affect the early pupal ecdysone synthesis. Alternatively, a global expression of Dilp8 may not have the same consequence in terms of viability as that of expression in a specific tissue since as reported earlier (*29*), global expression delays pupation and causes adults to be overweight because every tissue is equally affected. On the other hand, our experimental conditions up-regulate Dilp8 only in specific cell types.

It is reported earlier (*13, 14, 27, 40, 41, 43*) that damage to developing discs activates JNK signaling which in turn activates Dilp8. Many earlier studies in *Drosophila* and mammalian cells have shown that activated Ras triggers Eiger (TNF) mediated JNK signaling (*30, 42, 44-49*). The complete nullification of the activated Ras effects by co-expression of RafRBDFLAG, a dominant negative suppressor of Ras signaling (*31*), further confirmed that the elevated Ras-signaling mediated damage to eye imaginal discs indeed triggered the JNK signaling as also revealed by our microarray, qRT-PCR and immunostaining data. It is interesting that while levels of *tak*^{1} transcripts, whose product specifically activates the JNK pathway (*50*) were not affected in any of the genotypes examined, those of its homolog Takl1 (*51*) were highly up-regulated in *sev-GAL4>UAS-Ras1*^{V12} *hsrω-RNAi* as well as *sev-GAL4>UAS-Ras1*^{V12} *EP3037* pupae, which may contribute to the observed elevated JNK signaling in these eye discs. Our findings that all the genotypes that show early pupal lethality had elevated p-JNK levels in eye discs and elevated Dilp8 in early pupal discs reinforce involvement of JNK signaling in the process of Dilp8 synthesis.

Since Ptth triggers prothoracic gland to synthesize ecdysone hormone (*52-54*), the observed reduction in levels of *ptth* transcripts in brain lobes of early dying pupae indicates that the higher Dilp8 secreted by the early pupal eye discs inhibits *ptth* expression in brain which results in reduced ecdysone synthesis in the prothoracic glands. Dlip8 has earlier been reported to delay Ptth synthesis via the Lgr3 receptor (*13, 14, 28, 29*). In this context, the presence of high levels of Dilp8 in the four pairs of cerebral neurons in 8-9Hr old pupa, whose axons project on

proximal region of prothoracic gland and the reduction in transcripts of Lgr3 receptors in brain lobes of early dying pupae is intriguing. Presence of Dilp8 protein in these neurons appears to be a normal developmental expression since an identical pattern was seen even in the absence of *sev-GAL4* or *GMR-GAL4* driven expression of activated Ras. It remains to be seen if the Dilp8 positive neurons seen in our study are also expressing Lgr3. Reasons for the reduction in the *lgr3* transcripts in brain lobes of early dying pupae are not clear but may reflect a negative feedback loop activated by enhanced Dilp8 signaling. Another intriguing observation was the presence of *dilp8* transcripts in brain and ventral ganglia of all genotypes and their elevation in early dying pupae. Earlier reports have reported Dilp8 signal peptide to be produced by imaginal discs (*13, 14*). However, the modENcode mRNA tissue seq and cell line seq data in flybase.org report a low expression of *dilp8* transcripts in CNS of third instar larvae and P8 pupal stage similar to that in normally developing larval imaginal discs (flybase.org/report/Fbgn0036690.html). It is also intriguing that while the *dilp8* transcripts were elevated in brain lobes, the Dilp8 protein levels did not show a parallel increase in the early dying pupae. This may be related to the post-transcriptional regulation of *dilp8* transcripts (*55*).

Together, our results show that the elevated JNK signaling in late larval eye discs, due either to ectopically expressed high activated Ras or Reaper or Tak1, leads them to secret more Dilp8 after pupariation. The early pupal death following elevated levels of Dilp8 in eye discs observed in the present study is novel since the literature available so far (*13, 14, 27, 40, 41, 43*) has suggested that a major role of Dilp8 is to delay ecdysone synthesis, so that larvae can attain a minimal level of growth and development before advancing to the pupal stage. We found levels of the JNK-pathway, *dilp8* and ecdysone biosynthesis pathway (*spookier* and *phantom*) transcripts in eye discs and prothoracic glands (Fig. 6) were not as much affected in third instar larval as in the early pupal eye discs. Unlike the earlier reported nearly 100 fold increase in *dilp8* transcript levels in larvae expressing mutant polarity or tumor inducing genes (*56, 57*), we found only ~2-fold increase in *dilp8* transcripts in late third instar *sev-GAL4>UAS-Ras1^{V12} hsrω-RNAi* and *sev-GAL4>UAS-Ras1^{V12} EP3037* or *GMR-GAL4>UAS-Ras1^{V12}* or *GMR-GAL4>UAS-rpr* or *GMR-GAL4>UAS-tak^{1}* eye discs. This modest increase may not be enough to inhibit ecdysone biosynthesis in prothoracic glands. On the other hand, the very high Dilp8 levels in the early pupal eye discs of early dying pupal genotypes correlates with the substantial reduction in transcripts of *ptth* in brain and of some of the Halloween genes in pupal prothoracic glands which would result in the observed reduced ecdysone titer in early pupae. Therefore, it appears that the damage caused by *GMR-GAL4* or *sev-GAL4* driven expression of the specific transgenes during the 3rd instar stage remains below the threshold required for significantly elevating Dilp8 secretion. Consequently the larva pupates as usual. However, as the *GMR-GAL4* or *sev-GAL4* driven damage and the consequent increase in JNK signaling continues, Dilp8 levels increase following pupation and suppress the next ecdysone peak in >8-9Hr pupae. Since at this stage, the organism cannot postpone development, death ensues.

Present study highlights the communication between epithelia and the CNS and other organs so that deregulation of epithelial signaling results in global developmental consequences through downstream events in other tissues.

Material and Methods

Fly stocks

All fly stocks and crosses were maintained on standard agar cornmeal medium at 24±1^{0}C. The following stocks were obtained from the Bloomington *Drosophila* Stock Centre: w^{1118}*; sev-GAL4; +* (no. 5793), w^{1118}*; UAS-GFP* (no. 1521), w^{1118}*; UAS-rpr* (no. 5824), w^{1118}*; UAS-tak1* (no. 58810), ecd^1 (no. 218) and w^{1118}*; UAS-Ras1*^{V12} (no. 4847). The other stocks, viz., w^{1118}*; GMR-GAL4* (*8*), w^{1118}*; UAS-hsrω-RNAi*^{3} (*4*), w^{1118}*; EP3037/TM6B* (*4*), w^{1118}*; GMR-GAL4; UAS-hsrω-RNAi*^{3}, w^{1118}*; GMR-GAL4; EP3037/TM6B,* w^{1118}*; Sp/CyO;* dco^2 *e/TM6B* and w^{1118}*; UAS-127Q* (*58*), were available in the laboratory. The *UAS-hsrω-RNAi*^{3} is a transgenic line for down regulating the hsrω-nuclear transcripts while the *EP3037* allele over-expresses *hsrω* gene under a GAL4 driver (*4*). The *UAS-RafRBDFLAG* stock (*31*) was provided by Dr S Sanyal (Emory University, USA). Using these stocks, appropriate crosses were made to generate following stocks:

a) w^{1118}*; sev-GAL4 UAS-GFP;* dco^2 *e/TM6B*
b) w^{1118}*; sev-GAL4 UAS-GFP; UAS-hsrω-RNAi*^{3}
c) w^{1118}*; sev-GAL4 UAS-GFP; EP3037/TM6B*
d) w^{1118}*; UAS-GFP; UAS-Ras1*^{V12}
e) w^{1118}*; sev-GAL4 UAS-GFP;* ecd^1
f) w^{1118}*; UAS-RafRBDFLAG; UAS-Ras1*^{V12}*/TM6B*

Some of these were used directly or were further crossed to obtain progenies of following genotypes as required:

a) w^{1118}; sev-GAL4 *UAS-GFP/UAS-GFP;* dco^2 *e/+*
b) w^{1118}*; sev-GAL4 UAS-GFP/UAS-GFP;* dco^2 *e/UAS-Ras1*^{V12}
c) w^{1118}*; sev-GAL4 UAS-GFP/UAS-GFP; UAS-hsrω-RNA*$^{i3/}$*UAS-Ras1*^{V12}
d) w^{1118}*; sev-GAL4 UAS-GFP/UAS-GFP; EP3037/ UAS-Ras1*^{V12}
e) w^{1118}; sev-GAL4 *UAS-GFP/UAS-RafRBDFLAG;* dco^2 *e/+*
f) w^{1118}*; sev-GAL4 UAS-GFP/UAS-RafRBDFLAG;* dco^2 *e/UAS-Ras1*^{V12}
g) w^{1118}*; sev-GAL4 UAS-GFP/UAS-RafRBDFLAG; UAS-hsrω-RNAi*^{3}*/UAS-Ras1*^{V12}
h) w^{1118}*; sev-GAL4 UAS-GFP/UAS-RafRBDFLAG; EP3037/UAS-Ras1*^{V12}
i) w^{1118}*; GMR-GAL4/UAS-GFP*
j) w^{1118}*;GMR-GAL4/UAS-GFP; +/ UAS-Ras1*^{V12}
k) w^{1118}*;GMR-GAL4/UAS-GFP; UAS-hsrω-RNAi*^{3}*/ UAS-Ras1*^{V12}
l) w^{1118}*;GMR-GAL4/UAS-GFP; EP3037/ UAS-Ras1*^{V12}
m) w^{1118}*; GMR-GAL4/UAS-rpr*

n) *w^{1118}; GMR-GAL4/UAS-Tak1*
o) *w^{1118}; GMR-GAL4/UAS-127Q*.

The *w^{1118}*, *dco^2 e* and *UAS-GFP* markers are not mentioned while writing genotypes in Results while the *UAS-hsrω-RNAi^3* transgene (*4*) is referred to as *hsrω-RNAi*.

For conditional inhibition of ecdysone synthesis using the temperature-sensitive *ecd^1* mutant allele (*20*), the freshly formed *sev-GAL4 UAS-GFP; ecd^1* pupae, reared from egg-laying till pupation at 24±1^{0}C, were transferred to 30±1^{0}C for further development.

Flies of desired genotypes were crossed and their progeny eggs were collected at hourly intervals. Larvae that hatched during a period of 1Hr were separated to obtain synchronously growing larvae. Likewise, larvae that began pupation during an interval of 1Hr were separated to obtain pupae of defined age (expressed as Hr after pupa formation or Hr APF).

GFP imaging

Actively moving late third instar larvae and pupae of desired ages were dissected in Poels' salt solution (PSS) (*59*) and tissues fixed in 4% paraformaldehyde (PFA) in phosphate-buffered saline (PBS, 130 mm NaCl, 7 mm Na_2HPO_4, 3mm KH_2PO_4,pH 7.2) for 20 min. After three 10 min washes in 0.1% PBST (PBS + 0.1% Triton-X-100), the tissues were counterstained with DAPI (4', 6-diamidino-2-phenylindole dihydrochloride, 1µg/ml) and mounted in DABCO for imaging the *sev-GAL4* or *GMR-GAL4* driven *UAS-GFP* expression.

Whole organ immunostaining

Brain and eye discs from *sev-GAL4 UAS-GFP/UAS-GFP; dco^2e/+, sev-GAL4 UAS-GFP/UAS-GFP; dco^2 e/UAS-Ras1^{V12},sev-GAL4 UAS-GFP/UAS-GFP; UAS-hsrω-RNAi/UAS-Ras1^{V12},* and *sev-GAL4 UAS-GFP/UAS-GFP; EP3037/UAS-Ras1^{V12}* actively migrating late third instar larvae and pupae of desired age were dissected in PSS and immediately fixed in freshly prepared 4% paraformaldehyde in PBS for 20 min and processed for immunostaining as described earlier (*60*). The following primary antibodies were used: mouse monoclonal anti-Broad-core (1:50; DSHB, 25E9.D7), rabbit monoclonal anti-p-JNK (1:100; Promega) at and rat anti-Dilp8 (1:50; gifted by Dr. P. Léopold, France) (*14*). Appropriate secondary antibodies conjugated either with Cy3 (1:200, Sigma-Aldrich) or Alexa Fluor 633 (1:200; Molecular Probes) or Alexa Fluor 546 (1:200; Molecular Probes) were used to detect the given primary antibody. Chromatin was counterstained with DAPI (4', 6-diamidino-2-phenylindole dihydrochloride, 1µg/ml). Tissues were mounted in DABCO antifade mountant for confocal microscopy with Zeiss LSM Meta 510 using Plan-Apo 40X (1.3-NA) or 63X (1.4-NA) oil immersion objectives. Quantitative estimates of the proteins in different regions of eye discs were obtained with the help of Histo option of the Zeiss LSM Meta 510 software. All images were assembled using the Adobe Photoshop 7.0 software.

Measurement of ecdysone levels

Fifteen pupae of the desired stages and genotypes were collected in 1.5 ml tubes and stored at -70°C in methanol till further processing. They were homogenized in methanol and centrifuged at 13000 rpm following which the pellets were re-extracted in ethanol and air dried (*61*). The dried extracts were dissolved in EIA buffer at 4°C overnight prior to the enzyme immunoassay. The 20E-EIA antiserum (#482202), 20E AChE tracer (#482200), precoated (Mouse Anti-Rabbit IgG) EIA 96-Well Plates (#400007), and Ellman's Reagent (#400050) were obtained from Cayman Chemical, and assayed according to the manufacturer's instructions.

Microarray Analysis

RNA was isolated from 16-17Hr old *sev-GAL4>UAS-GFP*, *sev-GAL4>UAS-Ras1^{V12}*, *sev-GAL4>UAS-Ras1^{V12} hsrω*-RNAi and *sev-GAL4>UAS-Ras1^{V12} EP3037* pupae using TriReagent (Sigma-Aldrich) as per manufacturer's instructions. Microarray analysis of these RNA samples was performed on Affimetrix Drosophila Genome 2.0 microarray chips for 3' IVT array following the Affymetrix GeneChip Expression Analysis Technical manual using the GeneChip 3' IVT Plus Reagent Kit, Affymetrix GeneChip® Fluidics station 450, GeneChip® Hybridization oven 645 and GeneChip®Scanner 3000. Summary of the expression levels for each gene in the four genotypes was obtained from the Affymetrix Transcription analysis console and was subjected to Gene ontology search using David Bioinformatics software (https://**david**.ncifcrf.gov).The microarray data have been deposited at GEO repository (http://www.ncbi.nlm.nih.gov/geo/query/acc.cgi?acc=GSE80703).

Real Time Quantitative Reverse transcription–PCR (qRT-PCR)

Total RNAs were isolated from eye discs and brain ganglia of third instar larvae and appropriate pupal stages of the desired genotypes using TriReagent as per the manufacturer's (Sigma-Aldrich) instructions. First-strand cDNAs were synthesized as described earlier (*4*). The prepared cDNAs were subjected to real time PCR using forward and reverse primer pairs as listed in Table 4. Real time qPCR was performed using 5µl qPCR Master Mix (Syber Green, Thermo Scientific), 2 picomol/µl of each primer per reaction in 10 µl of final volume in ABI 7500 Real time PCR machine.

References

1. P. Ray, S. C. Lakhotia, Interaction of the non-protein-coding developmental and stress-inducible hsr omega gene with Ras genes of Drosophila melanogaster. *Journal of Biosciences* **23**, 377-386 (1998).
2. S. C. Lakhotia, Forty years of the 93D puff of Drosophila melanogaster. *J. Biosciences* **36**, 399-423 (2011).
3. F. D. Karim, H. C. Chang, M. Themen, D. A. Wassarman, T. Laverty, G. M. Rubin, A screen for genes that function downstream of Ras1 during Drosophila eye development. *Genetics* **143**, 315-329 (1996).
4. M. Mallik, S. Lakhotia, RNAi for the large non-coding hsr omega transcripts suppresses polyglutamine pathogenesis in *Drosophila* models. *Rna Biology* **6**, 464-478 (2009).
5. S. C. Lakhotia, M. Ray, Altered hsrω lncRNA levels in activated Ras background further enhance Ras activity in Drosophila eye and induces more R7 photoreceptors. *bioRxiv*, 224543 (2017).

6. E. J. Morris, W. A. Michaud, J.-Y. Ji, N.-S. Moon, J. W. Rocco, N. J. Dyson, Functional identification of Api5 as a suppressor of E2F-dependent apoptosis in vivo. *PLoS Genet* **2**, e196 (2006).
7. L. C. Firth, W. Li, H. Zhang, N. E. Baker, Analyses of RAS regulation of eye development in Drosophila melanogaster. *Methods in enzymology* **407**, 711-721 (2006).
8. M. Freeman, Reiterative use of the EGF receptor triggers differentiation of all cell types in the Drosophila eye. *Cell* **87**, 651-660 (1996).
9. D. D. Bowtell, T. Lila, W. M. Michael, D. Hackett, G. M. Rubin, Analysis of the enhancer element that controls expression of sevenless in the developing Drosophila eye. *Proc Natl Acad Sci U S A* **88**, 6853-6857 (1991).
10. A. Maixner, T. P. Hecker, Q. N. Phan, D. A. Wassarman, A screen for mutations that prevent lethality caused by expression of activated sevenless and Ras1 in the Drosophila embryo. *Developmental genetics* **23**, 347-361 (1998).
11. T.-K. Sang, G. Jackson, Drosophila models of neurodegenerative disease. *NeuroRx : the journal of the American Society for Experimental NeuroTherapeutics* **2**, 438-446 (2005).
12. M. Ray, S. C. Lakhotia, The commonly used eye-specific sev-GAL4 and GMR-GAL4 drivers in Drosophila melanogaster are expressed in tissues other than eyes also. *Journal of genetics* **94**, 407-416 (2015).
13. A. Garelli, A. M. Gontijo, V. Miguela, E. Caparros, M. Dominguez, Imaginal discs secrete insulin-like peptide 8 to mediate plasticity of growth and maturation. *Science* **336**, 579-582 (2012).
14. J. Colombani, D. S. Andersen, P. Léopold, Secreted peptide Dilp8 coordinates Drosophila tissue growth with developmental timing. *Science* **336**, 582-585 (2012).
15. D. R. Nässel, O. I. Kubrak, Y. Liu, J. Luo, O. V. Lushchak, Factors that regulate insulin producing cells and their output in Drosophila. *Frontiers in Physiology* **4**, (2013).
16. A. M. Handler, Ecdysteroid titers during pupal and adult development in Drosophila melanogaster. *Dev Biol* **93**, 73-82 (1982).
17. S. Zollman, D. Godt, G. G. Prive, J.-L. Couderc, F. A. Laski, The BTB domain, found primarily in zinc finger proteins, defines an evolutionarily conserved family that includes several developmentally regulated genes in Drosophila. *Proceedings of the National Academy of Sciences* **91**, 10717-10721 (1994).
18. B. Zhou, D. W. Williams, J. Altman, L. M. Riddiford, J. W. Truman, Temporal patterns of broad isoform expression during the development of neuronal lineages in Drosophila. *Neural development* **4**, 1 (2009).
19. I. F. Emery, V. Bedian, G. M. Guild, Differential expression of Broad-Complex transcription factors may forecast tissue-specific developmental fates during Drosophila metamorphosis. *Development* **120**, 3275-3287 (1994).
20. V. C. Henrich, R. L. Tucker, G. Maroni, L. I. Gilbert, The ecdysoneless (ecd1ts) mutation disrupts ecdysteroid synthesis autonomously in the ring gland of Drosophila melanogaster. *Developmental biology* **120**, 50-55 (1987).
21. A. Ragab, T. Buechling, V. Gesellchen, K. Spirohn, A. L. Boettcher, M. Boutros, Drosophila Ras/MAPK signalling regulates innate immune responses in immune and intestinal stem cells. *The EMBO journal* **30**, 1123-1136 (2011).
22. T. Hauling, R. Krautz, R. Markus, A. Volkenhoff, L. Kucerova, U. Theopold, A Drosophila immune response against Ras-induced overgrowth. *Biology open*, BIO20146494 (2014).
23. S. C. Lakhotia, Non-coding RNAs have key roles in cell regulation. *Proc. Indian Natn. Sci. Acad.* **82**, 1171-1182 (2016).
24. M. Mallik, S. C. Lakhotia, The developmentally active and stress-inducible noncoding *hsromega* gene is a novel regulator of apoptosis in *Drosophila*. *Genetics* **183**, 831-852 (2009).
25. X. Huang, J. T. Warren, L. I. Gilbert, New players in the regulation of ecdysone biosynthesis. *Journal of Genetics and Genomics* **35**, 1-10 (2008).

26. J. T. Warren, A. Petryk, G. Marqués, M. Jarcho, J.-P. Parvy, C. Dauphin-Villemant, M. B. O'Connor, L. I. Gilbert, Molecular and biochemical characterization of two P450 enzymes in the ecdysteroidogenic pathway of Drosophila melanogaster. *Proceedings of the National Academy of Sciences* **99**, 11043-11048 (2002).
27. A. Garelli, F. Heredia, A. P. Casimiro, A. Macedo, C. Nunes, M. Garcez, A. R. M. Dias, Y. A. Volonte, T. Uhlmann, E. Caparros, Dilp8 requires the neuronal relaxin receptor Lgr3 to couple growth to developmental timing. *Nature communications* **6**, 8732 (2015).
28. J. Colombani, D. S. Andersen, L. Boulan, E. Boone, N. Romero, V. Virolle, M. Texada, P. Léopold, Drosophila Lgr3 couples organ growth with maturation and ensures developmental stability. *Current Biology* **25**, 2723-2729 (2015).
29. D. M. Vallejo, S. Juarez-Carreño, J. Bolivar, J. Morante, M. Dominguez, A brain circuit that synchronizes growth and maturation revealed through Dilp8 binding to Lgr3. *Science* **350**, aac6767 (2015).
30. A. Minden, A. Lin, M. McMahon, C. Lange-Carter, B. Dérijard, R. J. Davis, G. L. Johnson, M. Karin, Differential activation of ERK and JNK mitogen-activated protein kinases by Raf-1 and MEKK. *Science* **266**, 1719-1723 (1994).
31. A. Freeman, M. Bowers, A. V. Mortimer, C. Timmerman, S. Roux, M. Ramaswami, S. Sanyal, A new genetic model of activity-induced Ras signaling dependent pre-synaptic plasticity in Drosophila. *Brain research* **1326**, 15-29 (2010).
32. N. Silverman, R. Zhou, R. L. Erlich, M. Hunter, E. Bernstein, D. Schneider, T. Maniatis, Immune activation of NF-κB and JNK requires Drosophila TAK1. *Journal of Biological Chemistry* **278**, 48928-48934 (2003).
33. P. Geuking, R. Narasimamurthy, B. Lemaitre, K. Basler, F. Leulier, A non-redundant role for Drosophila Mkk4 and hemipterous/Mkk7 in TAK1-mediated activation of JNK. *PloS one* **4**, e7709 (2009).
34. B. Stronach, Dissecting JNK signaling, one KKKinase at a time. *Dev Dyn* **232**, 575-584 (2005).
35. C. R. Weston, R. J. Davis, The JNK signal transduction pathway. *Current Opinion in Genetics & Development* **12**, 14-21 (2002).
36. T. Komura-Kawa, K. Hirota, Y. Shimada-Niwa, R. Yamauchi, M. Shimell, T. Shinoda, A. Fukamizu, M. B. O'Connor, R. Niwa, The Drosophila zinc finger transcription factor Ouija board controls ecdysteroid biosynthesis through specific regulation of spookier. *PLoS Genet* **11**, e1005712 (2015).
37. V. C. Henrich, M. D. Pak, L. I. Gilbert, Neural factors that stimulate ecdysteroid synthesis by the larval ring gland ofDrosophila melanogaster. *Journal of Comparative Physiology B* **157**, 543-549 (1987).
38. Y. S. Niwa, R. Niwa, Neural control of steroid hormone biosynthesis during development in the fruit fly Drosophila melanogaster. *Genes & genetic systems* **89**, 27-34 (2014).
39. A.-K. Claudius, P. Romani, T. Lamkemeyer, M. Jindra, M. Uhlirova, Unexpected role of the steroid-deficiency protein ecdysoneless in pre-mRNA splicing. *PLoS Genet* **10**, e1004287 (2014).
40. Y. Demay, J. Perochon, S. Szuplewski, B. Mignotte, S. Gaumer, The PERK pathway independently triggers apoptosis and a Rac1/Slpr/JNK/Dilp8 signaling favoring tissue homeostasis in a chronic ER stress Drosophila model. *Cell death & disease* **5**, e1452 (2014).
41. T. Katsuyama, F. Comoglio, M. Seimiya, E. Cabuy, R. Paro, During Drosophila disc regeneration, JAK/STAT coordinates cell proliferation with Dilp8-mediated developmental delay. *Proceedings of the National Academy of Sciences* **112**, E2327-E2336 (2015).
42. D. S. Andersen, J. Colombani, V. Palmerini, K. Chakrabandhu, E. Boone, M. Röthlisberger, J. Toggweiler, K. Basler, M. Mapelli, A.-O. Hueber, The Drosophila TNF receptor Grindelwald couples loss of cell polarity and neoplastic growth. *Nature* **522**, 482-486 (2015).
43. M. Zimmermann, S. J. Kugler, A. Schulz, A. C. Nagel, Loss of putzig Activity Results in Apoptosis during Wing Imaginal Development in Drosophila. *PloS one* **10**, e0124652 (2015).

44. M. Uhlirova, H. Jasper, D. Bohmann, Non-cell-autonomous induction of tissue overgrowth by JNK/Ras cooperation in a Drosophila tumor model. *Proceedings of the National Academy of Sciences of the United States of America* **102**, 13123-13128 (2005).
45. M. Wu, J. C. Pastor-Pareja, T. Xu, Interaction between RasV12 and scribbled clones induces tumour growth and invasion. *Nature* **463**, 545-548 (2010).
46. S. Ohsawa, Y. Sato, M. Enomoto, M. Nakamura, A. Betsumiya, T. Igaki, Mitochondrial defect drives non-autonomous tumour progression through Hippo signalling in Drosophila. *Nature* **490**, 547-551 (2012).
47. P. Khoo, K. Allan, L. Willoughby, A. M. Brumby, H. E. Richardson, In Drosophila, RhoGEF2 cooperates with activated Ras in tumorigenesis through a pathway involving Rho1–Rok–Myosin-II and JNK signalling. *Disease Models and Mechanisms* **6**, 661-678 (2013).
48. W. O. Miles, N. J. Dyson, J. A. Walker, Modeling tumor invasion and metastasis in Drosophila. *Disease Models and Mechanisms* **4**, 753-761 (2011).
49. C. I. Jones, A. L. Pashler, B. P. Towler, S. R. Robinson, S. F. Newbury, RNA-seq reveals post-transcriptional regulation of Drosophila insulin-like peptide dilp8 and the neuropeptide-like precursor Nplp2 by the exoribonuclease Pacman/XRN1. *Nucleic acids research* **44**, 267-280 (2016).
50. Y. Takatsu, M. Nakamura, M. Stapleton, M. C. Danos, K. Matsumoto, M. B. O'Connor, H. Shibuya, N. Ueno, TAK1 participates in c-Jun N-terminal kinase signaling during Drosophila development. *Mol Cell Biol* **20**, 3015-3026 (2000).
51. G. Manning, G. D. Plowman, T. Hunter, S. Sudarsanam, Evolution of protein kinase signaling from yeast to man. *Trends in biochemical sciences* **27**, 514-520 (2002).
52. Z. McBrayer, H. Ono, M. Shimell, J.-P. Parvy, R. B. Beckstead, J. T. Warren, C. S. Thummel, C. Dauphin-Villemant, L. I. Gilbert, M. B. O'Connor, Prothoracicotropic hormone regulates developmental timing and body size in Drosophila. *Developmental Cell* **13**, 857-871 (2007).
53. K. F. Rewitz, N. Yamanaka, L. I. Gilbert, M. B. O'Connor, The insect neuropeptide PTTH activates receptor tyrosine kinase torso to initiate metamorphosis. *Science* **326**, 1403-1405 (2009).
54. N. Yamanaka, K. F. Rewitz, M. B. O'Connor, Ecdysone control of developmental transitions: lessons from Drosophila research. *Annual Review of Entomology* **58**, 497-516 (2013).
55. C. I. Jones, A. L. Pashler, B. P. Towler, S. R. Robinson, S. F. Newbury, RNA-seq reveals post-transcriptional regulation of Drosophila insulin-like peptide dilp8 and the neuropeptide-like precursor Nplp2 by the exoribonuclease Pacman/XRN1. *Nucleic acids research* **44**, 267-280 (2015).
56. A. Figueroa-Clarevega, D. Bilder, Malignant Drosophila tumors interrupt insulin signaling to induce cachexia-like wasting. *Developmental Cell* **33**, 47-55 (2015).
57. B. D. Bunker, T. T. Nellimoottil, R. M. Boileau, A. K. Classen, D. Bilder, The transcriptional response to tumorigenic polarity loss in Drosophila. *Elife* **4**, e03189 (2015).
58. P. Kazemi-Esfarjani, S. Benzer, Genetic suppression of polyglutamine toxicity in Drosophila. *Science* **287**, 1837-1840 (2000).
59. M. Tapadia, S. Lakhotia, Specific induction of the hsr omega locus of Drosophila melanogaster by amides. *Chromosome Research* **5**, 359-362 (1997).
60. K. Prasanth, T. Rajendra, A. Lal, S. Lakhotia, Omega speckles - a novel class of nuclear speckles containing hnRNPs associated with noncoding hsr-omega RNA in *Drosophila*. *J. Cell Sci.* **113 Pt 19**, 3485-3497 (2000).
61. Q. Ou, A. Magico, K. King-Jones, Nuclear receptor DHR4 controls the timing of steroid hormone pulses during Drosophila development. *PLoS Biol* **9**, e1001160 (2011).

Figures and Legends

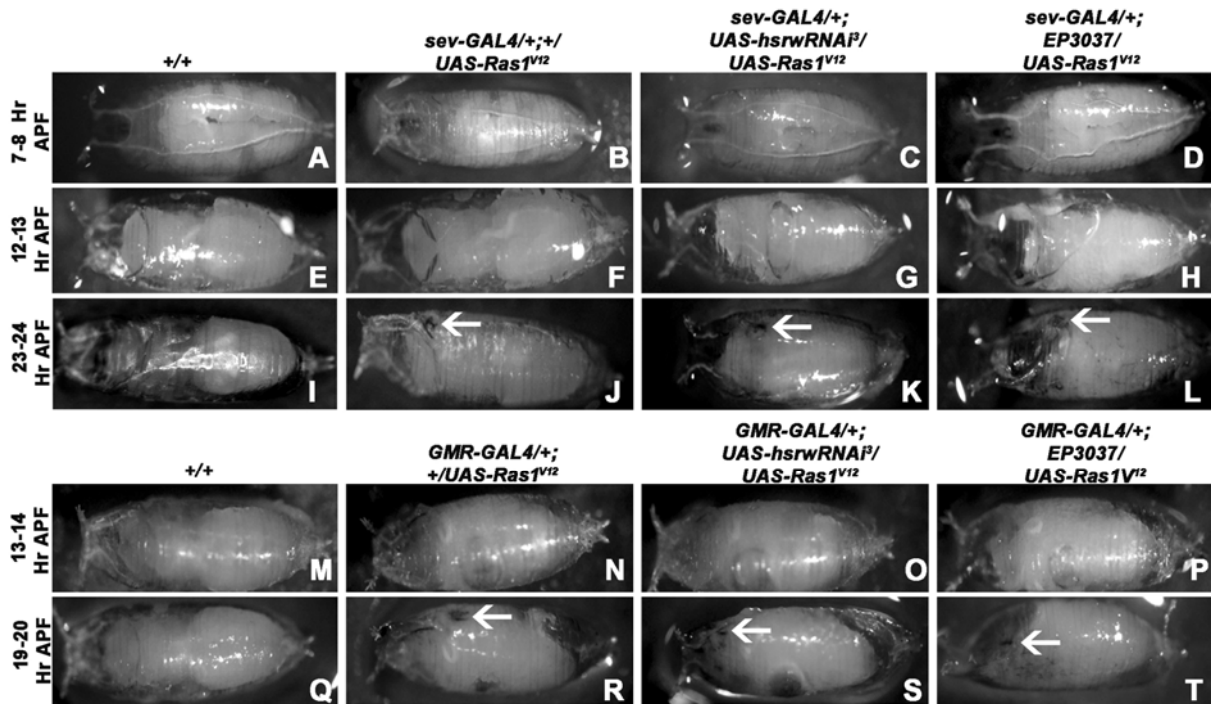

Fig. 1. ***sev-GAL4*** **or** ***GMR-GAL4*** **driven expression of activated Ras together with altered hsrω-n transcript levels leads to early pupal lethality accompanied by absence of prepupal to pupal metamorphic changes.** (**A-T**) Photomicrographs of pupae at different stages of development (noted on left of each row) in different genotypes (noted on top of the columns). White arrows in **J**-**L** and **R**-**T** indicate the necrotic patch near eye region.

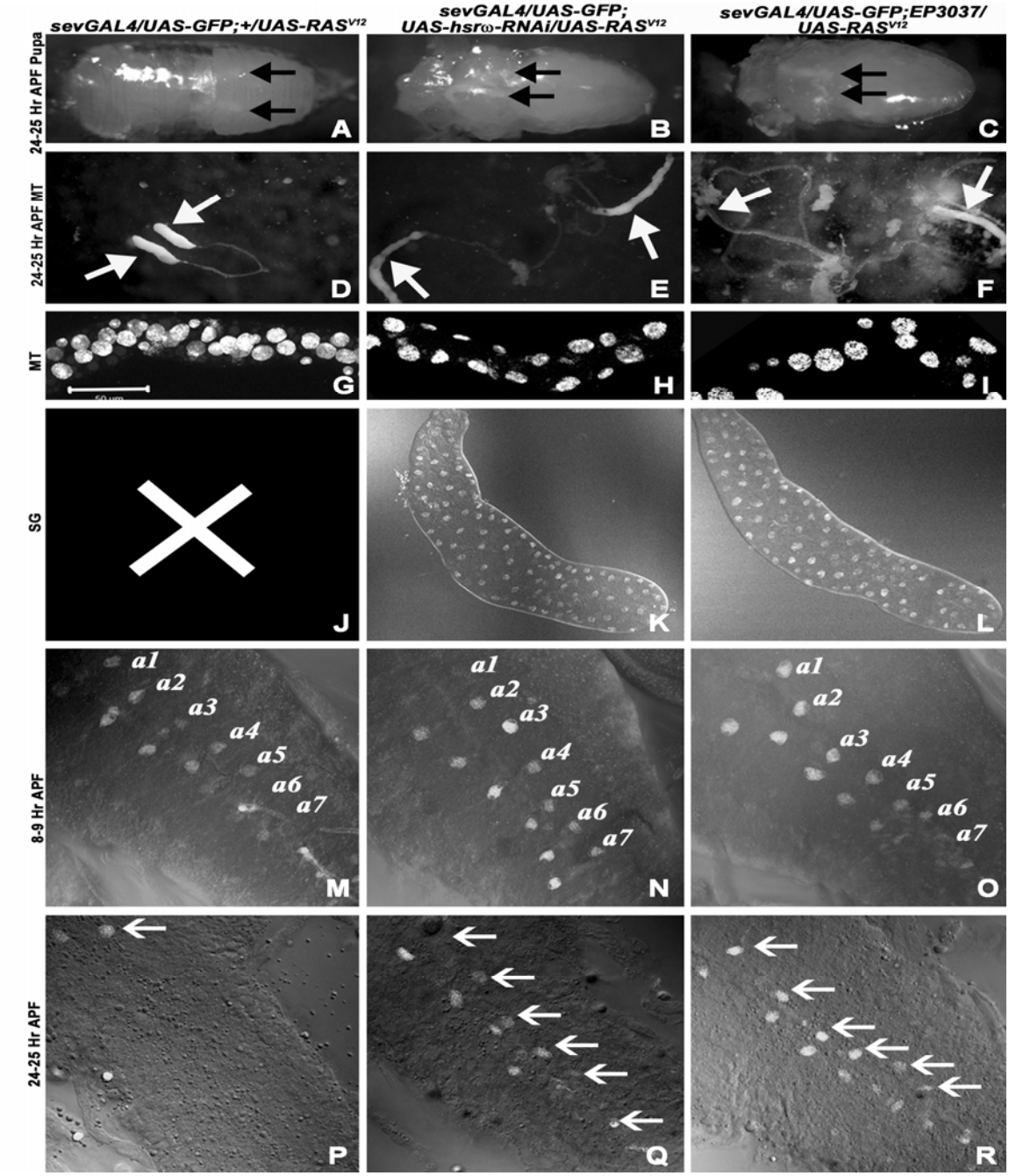

Fig. 2. The prepupal to pupal metamorphic changes in internal organs are affected in early dying pupae. 24-25Hr old pupae (**A-C**) and dissected out anterior Malpighian tubules (**D-F**) of genotypes noted above each column. White arrows in **D-F** indicate the distal segments of anterior Malpighian tubules. (**G-L**) Confocal optical sections of DAPI stained Malpighian tubules (**G-I**) and salivary glands (**J-L**) of 24-25Hr pupae; a cross is marked at **J** as salivary glands are no longer seen at 24-25Hr APF in *sev-GAL4>UAS-Ras1*^{V12}. (**M-R**) Confocal projections of ventral ganglia showing *sev-GAL4*>UAS-GFP expressing (white) dorso-medial segmental paired neurons in abdominal segments (**a1** to **a7**, arrows) at 8-9Hr APF (**M-O**) and at 24-25Hr APF (**P-R**) stages in different genotypes noted above each column. Scale bar in **G** is 50µm and applies to **G-R**.

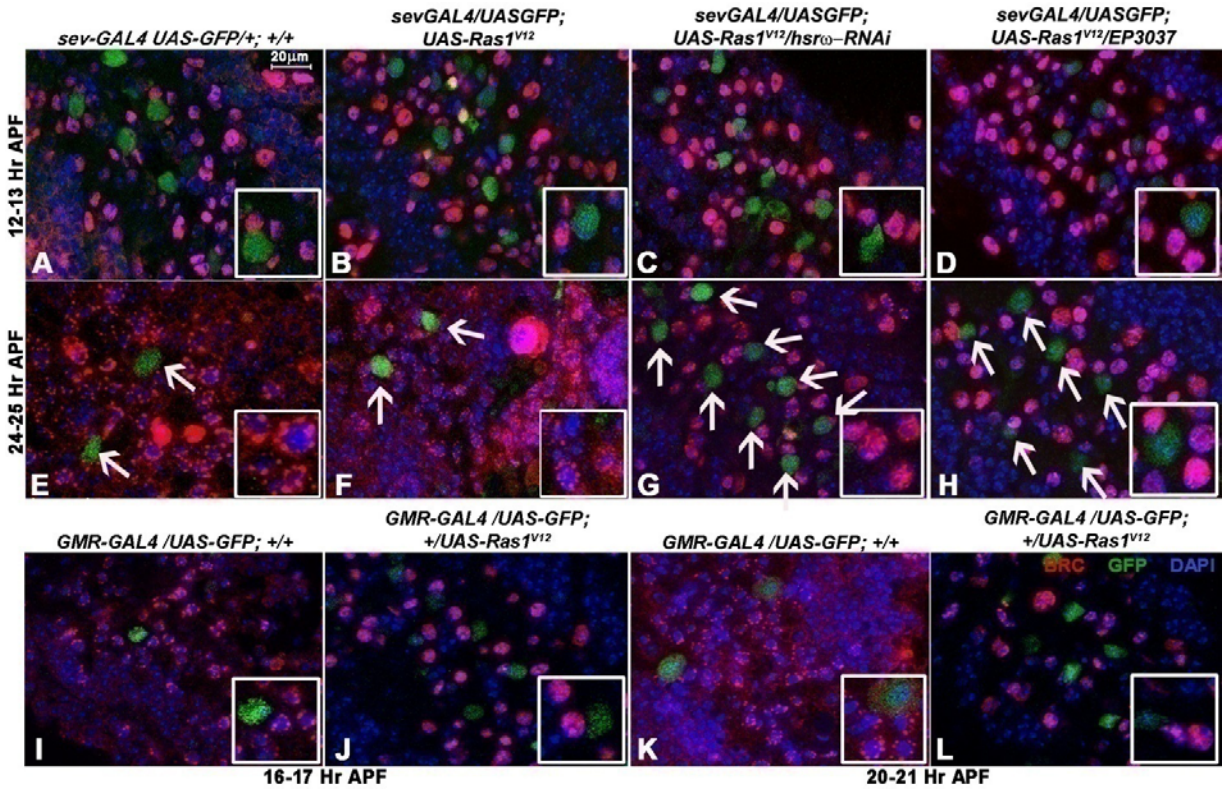

Fig. 3. Distribution of Broad protein in ventral ganglia cells at 16-17Hr or later APF is affected in early dying pupae. (**A-H**) Confocal optical sections showing parts of ventral ganglia from 12-13Hr (**A-D**) and 24-25Hr (**E-H**) old pupae immunostained with anti-Broad-core (red) and counterstained with DAPI (blue); GFP (green) marks the *sev-GAL4* expressing neurons (also indicated by white arows). Genotypes are noted above each column. (**I-L)** Confocal optical sections of parts of ventral ganglia from 16-17Hr (**I, J**) and 20-21Hr (**K, L**) old pupae (genotypes noted above each image) immunostained with anti-Broad-core (red), counterstained and with DAPI (blue); GFP (green) marks the *GMR-GAL4* expressing neurons. Inset in each panel shows higher magnification images of a few Broad expressing cells. Scale bar in (**A**) indicates 20µm and applies to all images.

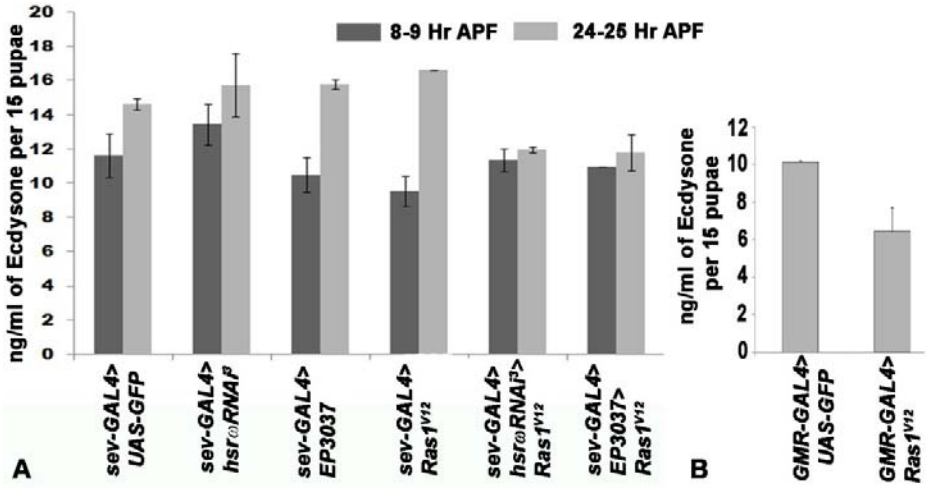

Fig. 4. **The expected increase in ecdysone levels in post 8-9Hr pupae does not occur in pupae that are destined to die early. A-B** Histograms showing mean (±S.E. of two independent replicates) levels of 20 hydroxy-ecdysone (Y axis) in different genotypes (X-axis) at 8-9Hr APF (dark grey) and at 24-25Hr APF stages (light grey). Each genotype also carries *UAS-GFP* transgene.

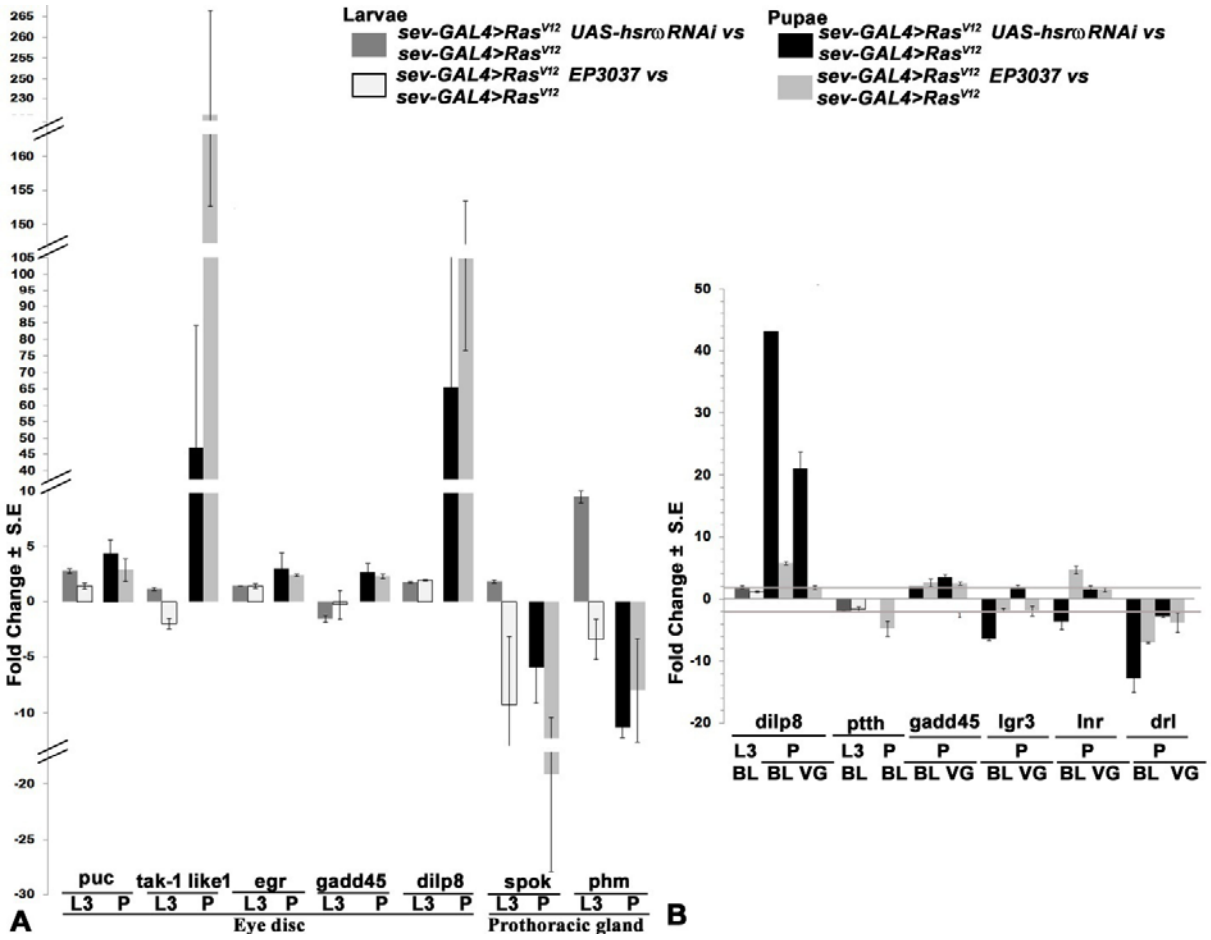

Fig. 5. Transcript levels of some JNK pathway, *dilp8*, *ptth* and ecdysone biosynthesis pathway Halloween genes changed significantly at early pupal but not late larval stages in genotypes showing early pupal death. A Histograms showing qRT-PCR based mean fold changes (±S.E., Y-axis) in levels of different transcripts in eye discs or prothoracic glands (X-axis) of *sev-GAL4>UAS-Ras1^{V12} hsrω-RNAi* and *sev-GAL4>UAS-Ras1^{V12} EP3037* late 3rd instar larvae (L3) or 8-9Hr old pupae (P) when compared with those expressing only activated Ras under *sev-GAL4* driver. **B** Histograms showing qRT-PCR based mean (±S.E.) fold changes (Y-axis) in levels of different transcripts (X-axis) in brain lobes (BL) or ventral ganglia (VG) of *sev-GAL4>UAS-Ras1^{V12} hsrω-RNAi* and *sev-GAL4>UAS-Ras1^{V12} EP3037* late 3rd instar larvae (L3) or 8-9Hr old pupae (P) when compared with those expressing only activated Ras under *sev-GAL4* driver. Grey lines mark the plus and minus two fold change compared to the controls. Keys for different bars are provided at top.

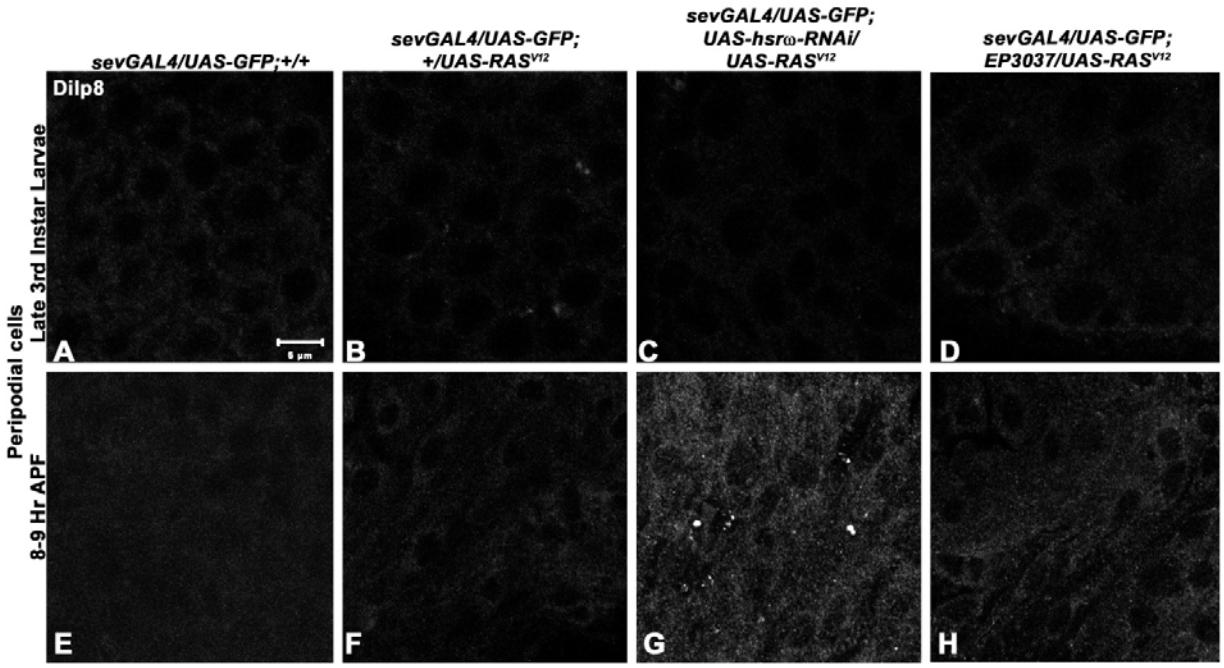

Fig 6. Expression of Dilp8 remains unchanged in eye discs of third instar larvae but increases in that of 8-9 Hr pupae of genotypes that show early pupal death. A-H Confocal single section images of third instar larval eye disc peripodial cells (**A-D**) and of 8-9 Hr pupae (**E-H**) showing Dilp8 (white) in different genotypes (noted on top of each column) . Scale bar in **A** denotes 5µm and applies to **A-H**.

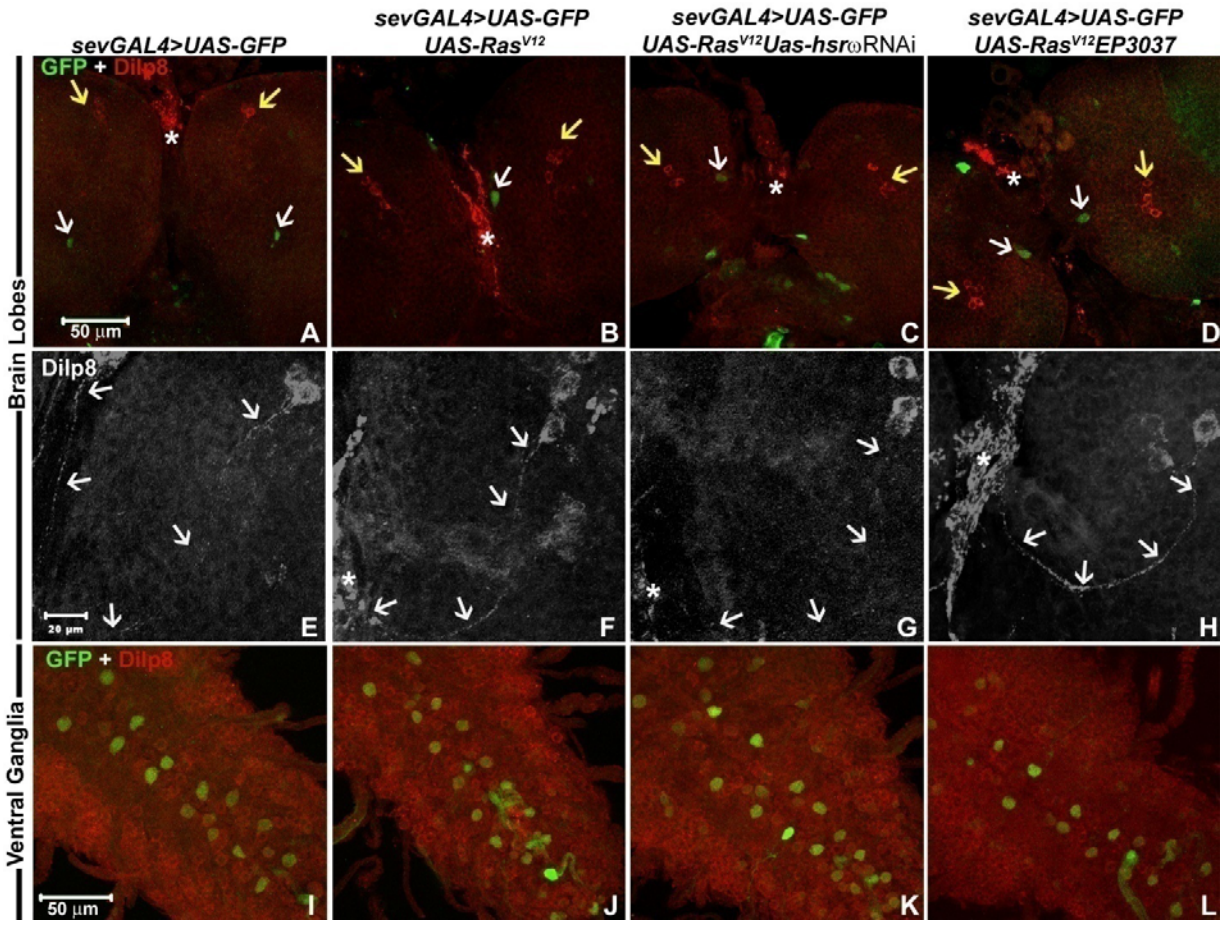

Fig. 7. Ectopic expression of activated Ras does not affect Dilp8 levels in brain lobes and ventral ganglia of 8-9 Hr old pupae. Confocal projection images of brain lobes (**A**-**H**) and ventral ganglia (**I**-**L**) of 8-9 Hr old pupae of different genotypes (noted on top of each column) showing Dilp8 (red in **A**-**D** and **I**-**L**, white in **E**-**H**) and *sev-GAL4>GFP* (green in **A**-**D** and **I**-**L**). White arrows in **A**-**D** indicate the GFP-positive neurons in antero-medial part of brain ganglia while the yellow arrows indicate the mid-lateral groups of four Dilp8 expressing neurons in each brain lobe; the basal region of prothoracic gland is marked by asterisk. **E**-**H** show higher magnification images of Dilp8 staining in one of the brain lobes with the white arrows indicating the Dilp8 positive axonal projections from the group of Dilp8 positive neurons to the basal region of prothoracic gland (marked by asterisk). The scale bar (50 µm) in **A** applies to **A**-**D** while that in **I** (20 µm) applies to **I**-**L**.

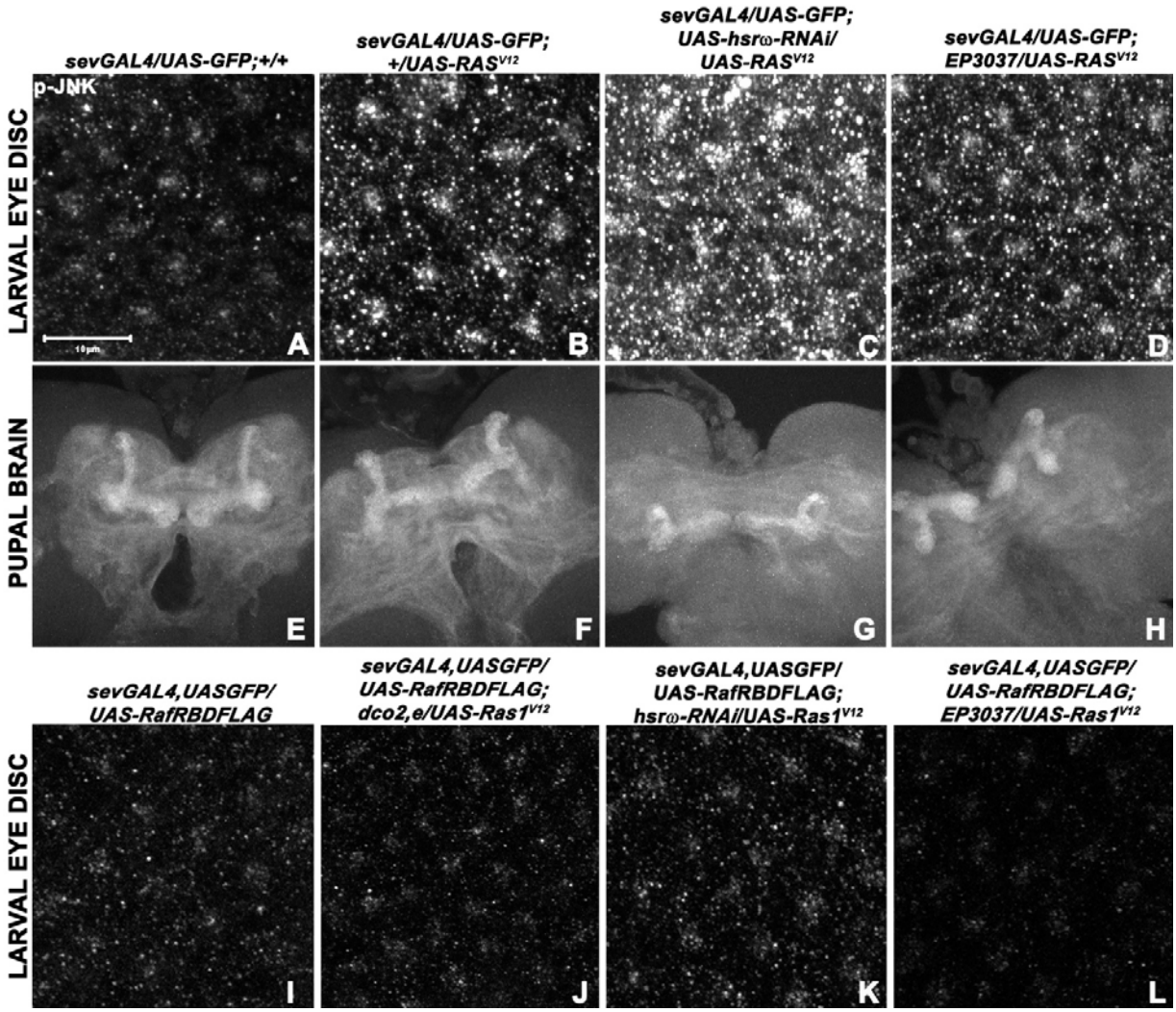

Fig. 8. **Expression of phosphorylated JNK (p-JNK) is enhanced in larval eye discs of early dying pupae due to ectopic Ras signaling. A-L** Confocal projection images of third instar larval eye discs (**A-D** and **I-L**) and 8-9 Hr pupal brain (**E-H**) showing p-JNK (white) in different genotypes (noted above the columns). Scale bar in **A** denotes 10µm and applies to **A-L.**

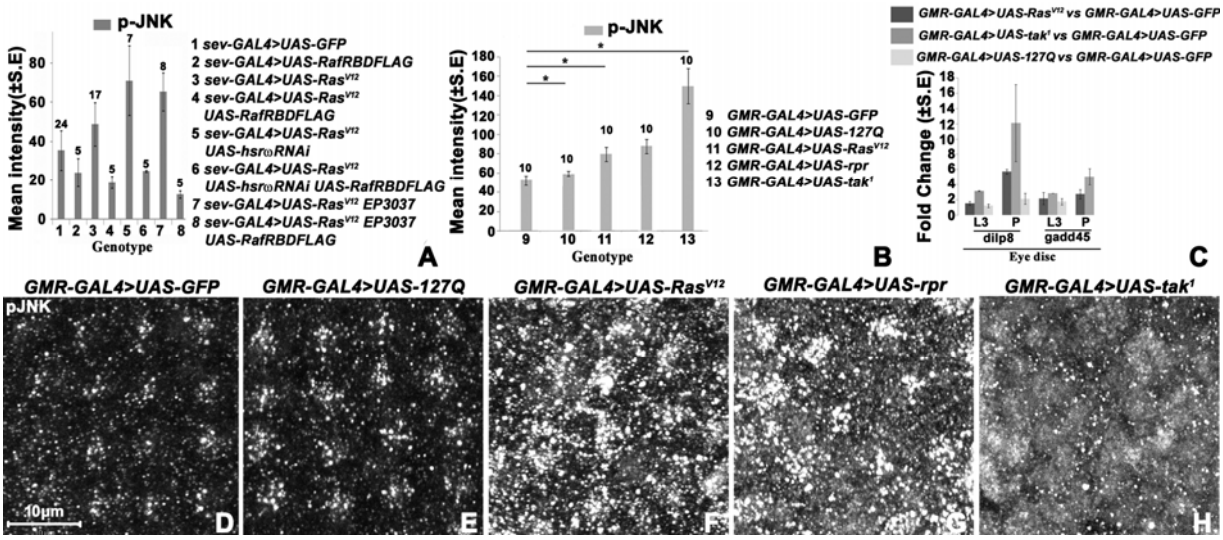

Fig. 9. **Expression of Dilp8 and phosphorylated JNK (p-JNK) is enhanced in eye discs of early dying pupae. A-B** Histograms showing mean (± S. E.) fluorescence intensity (Y-axis) of p-JNK in the eye discs of different genotypes (1-13, indexed on right side); number on top of each bar indicates the number of eye discs examined. **C** Histogram showing qRT-PCR based mean (±S.E. based on two biological replicates) fold changes (Y-axis) in levels of different transcripts (X-axis) in eye discs of *GMR-GAL4>UAS-Ras1^{V12}*(black bars), *GMR-GAL4$^{>UAS\text{-}tak1}$* (dark gray bars) and *GMR-GAL4>UAS-127Q* (light gray bars) late 3rd instar larvae (L3) or 8-9Hr old pupae (P) when compared to control *GMR-GAL4>UAS-GFP*. **D-H** Confocal projection images of parts of third instar larval eye discs in genotypes mentioned on top of each panel showing distribution of p-JNK. Scale bar in **D** denotes 10µm and applies to **D-H.**

Tables

Table 1. Exogenous ecdysone partially suppressed early pupal death in *sev-GAL4>UAS-GFP; ecd^{1}* (maintained at restrictive temperature from 0Hr pre-pupa onwards), *sev-GAL4>UAS-Ras1^{V12} hsrω-RNAi* and *sev-GAL4>UAS-Ras1^{V12} EP3037* pupae

Treatment	**Genotype**								
	***sev-GAL4>UAS-GFP; ecd^{1}* at 30^{0}C**			***sev-GAL4>UAS-Ras1^{V12} hsrω-RNAi* at 24^{0}C**			***sev-GAL4>UAS-Ras1^{V12} EP3037* at 24^{0}C**		
	N	**Early Pupal Death**	**Late Pupal Death**	**N**	**Early Pupal Death**	**Late Pupal Death**	**N**	**Early Pupal Death**	**Late Pupal Death**
a. Control	**43**	**54%**	**46%**	**49**	**82%**	**18%**	**38**	**71%**	**29%**
b. Ecdysone treatment*	**48**	**27%**	**73%**	**62**	**58%**	**42%**	**50**	**32%**	**68%**
Fold change in time of death (a/b)		**2 Fold decrease**			**1.4 Fold decrease**			**2.2 Fold decrease**	

* 8Hr old pupae incubated in ecdysone (1µg/ml) containing PBS for 12Hr at the indicated temperature following which they were blotted dry and monitored for their subsequent development.

N = total number of pupae examined

Table 2. Transcription of several genes in steroid and ecdysone biosynthesis, insulin- and JNK-signaling pathways was affected when levels of hsrω transcripts were co-altered with *sev-GAL4>Ras1^{V12}* expression

Genes	**Mean Fold changes in transcript levels between different pairs of genotypes**				
	sev-GAL4> Ras1^{V12} vs sev-GAL4>UAS-GFP	***sev-GAL4> Ras1^{V12} hsrω-RNAi vs sev-GAL4>UAS-GFP***	***sev-GAL4> Ras1^{V12} EP3037 vs sev-GAL4>UAS-GFP***	***sev-GAL4> Ras1^{V12} hsrω-RNAi vs sev-GAL4>UAS-Ras1^{V12}***	***sev-GAL4> Ras1^{V12} EP3037 vs sev-GAL4>UAS-Ras1^{V12}***
			Ecdysone Biosynthesis Pathway		
spok	2.55	-1.24	-1.81	-3.17	-4.62
phm	1.74	-1.18	-1.75	-2.06	-3.04
dib	-1.24	4.63	1.91	5.73	2.37
sad	1.65	-1.31	-1.65	-2.16	-2.71
shd	-1.11	1.35	-1.16	1.5	-1.05
			insulin pathway		
dilp1	1.21	1.48	-1.9	1.22	-2.31
dilp 2	-1.75	-1.11	-1.76	1.58	-1.01
dilp 3	1.65	1.28	-1.33	-1.29	-2.19
dilp 4	-1.09	1.59	-1.23	1.73	-1.13
dilp 5	-1.07	1.6	-1.92	1.71	-1.8

dilp 6	-1.24	1.18	-1.63	1.47	-1.32
dilp 7	-1.21	1.36	-1.28	1.65	-1.05
dilp 8	1.48	6.56	2.79	4.43	1.88
tobi	N. S.	8.08	2.83	5.34	1.87
lgr3	1.13	1.84	1.09	1.63	-1.04
			JNK Pathway		
bsk	1.71	1.96	-1.17	1.15	-2
CYLD	1.59	2.12	1.01	1.33	-1.58
dpp	1.27	2.49	-1.43	1.95	-1.82
egr	2.86	5.66	2.1	1.98	-1.36
gadd45	2.08	5.71	2.74	2.74	1.32
hep	1.28	1.56	-1.4	1.37	-1.59
Jra	1.48	2.31	1.08	1.56	-1.37
kay	-1.15	1.68	-1.49	1.93	-1.3
Mnn1	1.36	1.68	-1.61	1.23	-2.19
msn	1.11	2.16	-1.43	1.94	-1.59
NLaz	1.21	2.86	1.57	2.37	1.3
PSR	1.16	1.11	-1.77	-1.04	-2.04
puc	1.11	2.4	1.09	2.16	-1.02
pyd	-1.92	2.15	1.13	4.12	2.16
Rala	-3.29	-1.1	-2.91	3	1.13
raw	1.52	4.31	1.63	2.83	1.07
scaf	1.86	1.52	-1.3	-1.22	-2.41
src42A	1.27	1.56	-1.22	1.23	-1.56
src64B	1.94	3.2	1.26	1.65	-1.54
tak1	1.6	-1.1	-2.27	-1.75	-3.62
takl1	-1.58	7.84	2.59	12.37	4.08
traf-like	-1.46	1.68	-1.05	2.45	1.39
wnd	1.06	-1.08	-1.71	-1.15	-1.82

Note: the gray highlighted values indicate similar up-or down regulation in genotypes co-expressing *hsrω-RNAi* or *EP3037* with $Ras1^{V12}$

Table 3. Ras signaling dependent elevated p-JNK levels correlate with early pupal lethality

Genotype	**Pupal survival (N=500 or more for each genotype)**	**p-JNK levels in 3rd instar eye discs (relative to *GMR-GAL4>UAS-GFP* (rows 1-4) or *sev-GAL4>UAS-GFP* (rows 5-12))**	**Dilp8 levels in early pupal eye discs**
1. *GMR-GAL4>UAS-Ras1^{V12}*	100% Early pupal death	Very high	High
2. *GMR-GAL4>UAS-rpr*	100% Early pupal death	Very High	High
3. GMR-GAL4>UAS-tak1	100% Early pupal death	Very high	High
4. *GMR-GAL4>UAS-127Q*	100% survival to adult stage	Normal	Normal
5. sev-GAL4>UAS-GFP	100% survival to adult stage	Normal	Normal
6. sev-GAL4>UAS-Ras1^{V12}	88% Late pupal death; 12 % emerge as flies	Moderately high	Normal
7. *sev-GAL4>UAS-Ras1^{V12} hsrω-RNAi*	96% Early pupal death; 4% late pupal death ((5), Fig. 1)	Very high	High
8. *sev-GAL4>UAS-Ras1^{V12} EP3037*	42% Early pupal death; 58% late pupal death ((5)Fig. 1)	High	High
9. *sev-GAL4>RAFRBDFLAG*	100% survival to adult stage	Low	Not examined
10. *sev-GAL4>UAS-Ras1^{V12} RAFRBDFLAG*	100% survival to adult stage	Low	Not examined
11. *sev-GAL4>UAS-Ras1^{V12} RAFRBDFLAG hsrω-RNAi*	100% survival to adult stage	Low	Not examined
12. sev-GAL4>UAS-Ras1^{V12} RAFRBDFLAGEP3037	100% survival to adult stage	Low	Not examined

Shaded cells indicate correlation between early pupal death and very high p-JNK and Dilp8 levels in larval eye discs

Table 4. Forward and reverse primers used for qRT-PCR for quantification of different transcripts

Transcripts and Primers		SEQUENCE (5'-3')	AMPLICON SIZE
Spookier	*Forward*	TGCGACTGGTCTCAATTACAA	164 bp
	Reverse	TCACATGGATATCCCGAAGAA	
Phantom	*Forward*	CTTGCATTTCCGAGACGATG	150bp
	Reverse	CCACTGGGTCCATGTGGATA	
Tak1-like 1	*Forward*	ACCGATTGTTCACCGCGATA	229bp
	Reverse	TTGACGTGTCATCAGCTCCC	
Dilp 8	*Forward*	GGAGTGGGCACAAATAAGGT	153bp
	Reverse	TCTTTGGAAGTTGCCTCATTGG	
Eiger 2	*Forward*	GACGCGAACGGACGTTTAAA	228bp
	Reverse	TTTGCGATAAAGGCACAGCG	
Gadd45	*Forward*	GGGATCCCTCTTCTGCCTGA	121bp
	Reverse	GTCGTCCACCTTGATCACGT	
Puckered	*Forward*	TACAAGTCGCTCTCCCTGCT	196bp
	Reverse	GGGTGCTTAATCCCACAGAA	
G3PDH	*Forward*	AGGCGTTTGTGACTTCTGGA	129bp
	Reverse	TGTCCTCCAGACCCTTGTTC	
lgr3	*Forward*	GTCTCCTCTACGGCAGCAAG	102bp
	Reverse	CACCGCTCGCATTTGAAACG	
Inr	*Forward*	TGAAATCAGTGCGGAGGAGG	116bp
	Reverse	CGCTGCATTTAACGTCCCTC	
drl	*Forward*	TCCAGAGACTGCCCACCATA	206bp
	Reverse	CCCAAAGTTTCCCTCCTGGA	
ptth	*Forward*	AGGAATCGCCAGTCAGTACG	161bp
	Reverse	TCTCTGTGGGATGTGGAGTG	
Rp49	*Forward*	TTGAGAACGCAGGCGACCGT	91bp
	Reverse	CGTCTCCTCCAAGAAGCGCAAG	

Supplementary Material

Supplementary Figures & Legends

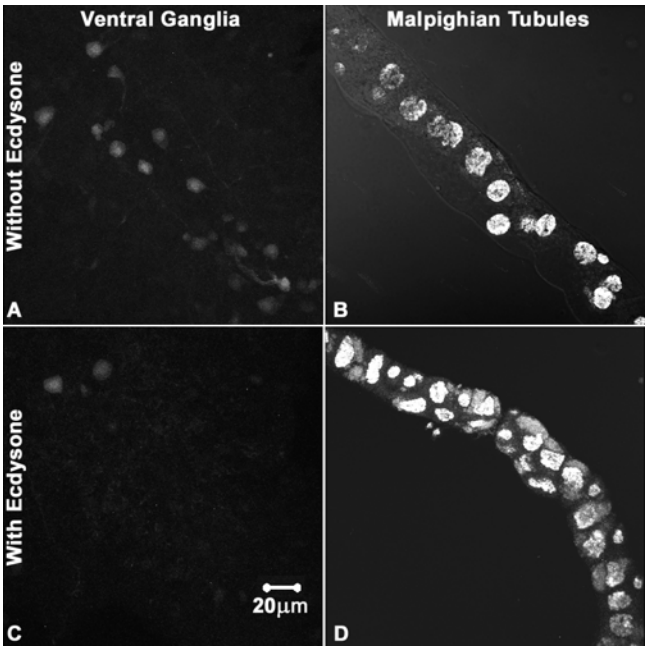

Fig. S1. Exogenous ecdysone promotes prepupal to pupal metamorphic changes in *ecd*^{1} mutant pupae maintained at the restrictive temperature (30^{0}C). (**A**, **C**) Confocal projection showing GFP (white) expression in ventral ganglia in 24-25Hr old *sevGAL4>UAS-GFP; ecd*^{1} pupae maintained at 30^{0}C since the beginning of pupation without (**A**) or with (**C**) exposure to exogenous ecdysone between 8-20Hr APF. (**B**, **D**) Confocal projection images of DAPI-stained (white) Malpighian tubules of 24-25Hr old *sevGAL4>UAS-GFP; ecd*^{1} pupae maintained at 30^{0}C since the beginning of pupation without (**B**) or with (**D**) exposure to exogenous ecdysone between 8-20Hr APF. The scale bar in **C** applies to all the images.

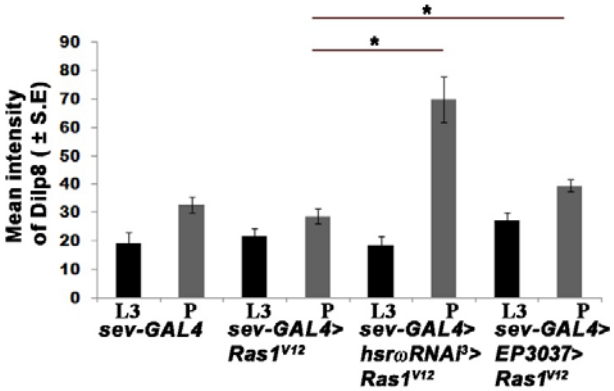

Fig. S2. Dilp8 protein is more abundant in 8-9Hr pupal than in third instar larval eye discs of genotypes that show early pupal death. Histograms showing mean intensity (±S.E.) levels of Dilp8 (Y axis) in different genotypes (X-axis) in late third instar larval (black) and 8-9 Hr pupal eye discs (grey). Each genotype also carries *UAS-GFP* transgene. 15 eye discs, from three independent replicates, were

examined for each genotype. Student's t-test was performed to compare different groups; none of them showed any significant difference except in two cases, indicated by an asterisk above the horizontal line connecting the compared genotypes, which showed significant difference ($P \leq 0.05$).

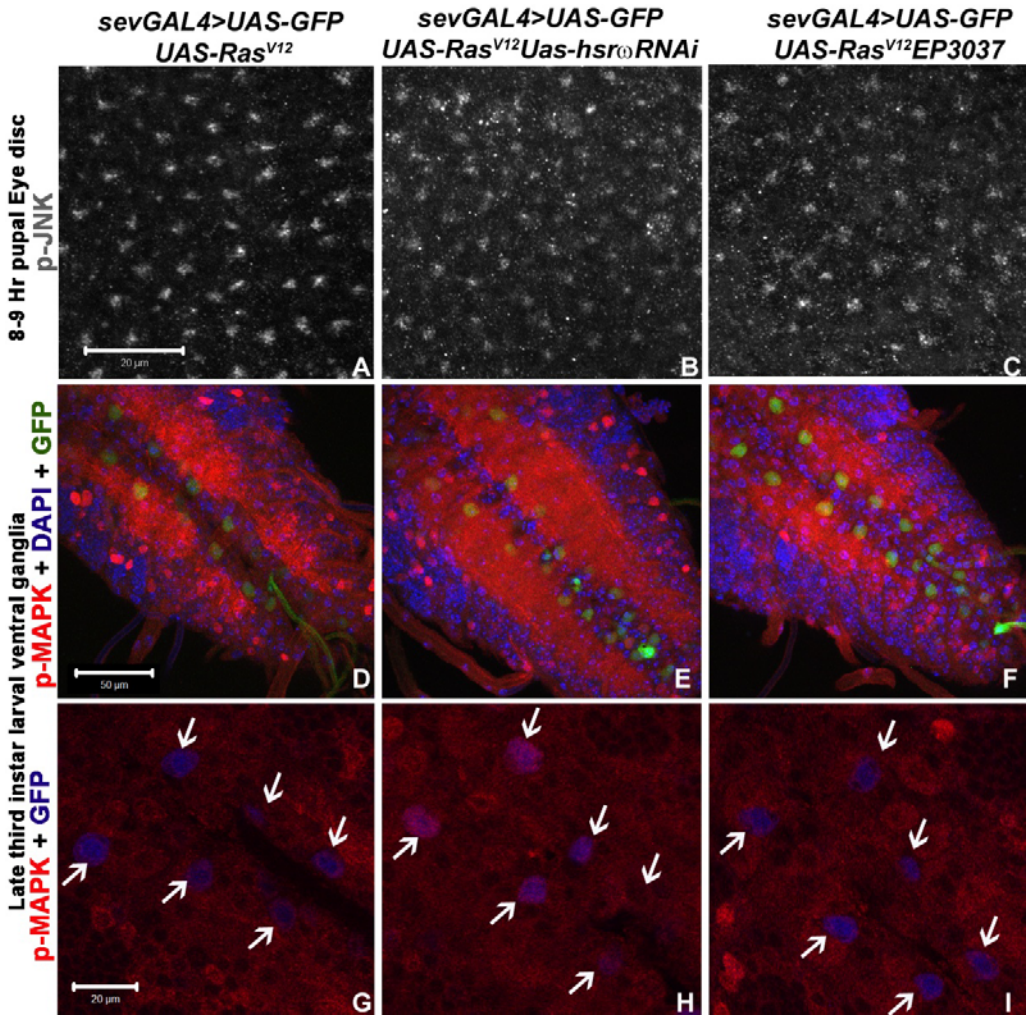

Fig. S3. p-JNK is elevated in 8-9 Hr pupal eye discs but there is insignificant change in overall p-MAPK level in larval CNS of individuals expressing *sev-GAL4* driven activated Ras without or with altered levels of *hsrω* transcripts. A-C Confocal projection images of 8-9 Hr old pupal eye discs immunostained for p-JNK (white) in genotypes mentioned at top of each column. **D-I** Confocal projection images (**D-F**) and single sections (**G-I**) of ventral ganglia in third instar larva showing presence of p-MAPK (red), counterstained with DAPI (blue in **D-F**). Cells expressing GFP under *sev-GAL4* are shown in green in **D-F** and in blue in **G-I** (marked with arrows). Scale bar in **A** (20µm) applies to **A-C,** in **D** (50 µm) applies to **D-F** and in **G** (20µm) applies to **G-I.**

Supplementary Table

Table S1. Major pathways affected in individuals co-expressing *sev-GAL4* driven activated Ras (*Ras1^{V12}*) and *EP3037*or activated Ras and *hsrω-RNAi* when compared with those expressing *sev-GAL4* driven activated Ras only.

Pathways commonly up-regulated in *sev-GAL4>UAS-Ras1^{V12}>EP3037* and *sev-GAL4>UAS-Ras1^{V12}>hsrω-RNAi*	**Pathways commonly down-regulated in *sev-GAL4>UAS-Ras1^{V12}>EP3037* and *sev-GAL4>UAS-Ras1^{V12}>hsrω-RNAi***	**Pathways down-regulated in *sev-GAL4>UAS-Ras1^{V12}>EP3037* but up-regulated in *sev-GAL4>UAS-Ras1^{V12}>hsrω-RNAi***	**Pathways down-regulated only in *sev-GAL4>UAS-Ras1^{V12}>EP3037***	**Pathways up-regulated only in *sev-GAL4>UAS-Ras1^{V12}>hsrω-RNAi***
GO:0006030: chitin metabolic process	GO:0008610: lipid biosynthetic process	GO:0007160: cell-matrix adhesion	GO:0051174: regulation of phosphorus metabolic process	GO:0042180: cellular ketone metabolic process
GO:0006022: aminoglycan metabolic process	GO:0005976: polysaccharide metabolic process	GO:0031589: cell-substrate adhesion	GO:0019220: regulation of phosphate metabolic process	GO:0006575: cellular amino acid derivative metabolic process
GO:0016052: carbohydrate catabolic process	GO:0006694: steroid biosynthetic process	GO:0007155: cell adhesion	GO:0055114: oxidation reduction	GO:0019471: 4-hydroxyproline metabolic process
GO:0005976: polysaccharide metabolic process	GO:0002376: immune system process	GO:0010631: epithelial cell migration	GO:0009101: glycoprotein biosynthetic process	GO:0043436: oxoacid metabolic process
GO:0006950: response to stress	GO:0045087: innate immune response	GO:0007165: signal transduction	GO:0046068: cGMP metabolic process	GO:0006082: organic acid metabolic process
GO:0009266: response to temperature stimulus		GO:0007188: G-protein signaling, coupled to cAMP nucleotide second messenger	GO:0035103: sterol regulatory element binding protein cleavage	GO:0019752: carboxylic acid metabolic process
GO:0009308: amine metabolic process		GO:0007187: G-protein signaling, coupled to cyclic nucleotide second messenger	GO:0007552: metamorphosis	GO:0007254: JNK cascade
GO:0005975: carbohydrate metabolic process		GO:0007166: cell surface receptor linked signal transduction	GO:0006334: nucleosome assembly	GO:0031098: stress-activated protein kinase signaling pathway
GO:0006629: lipid metabolic process		GO:0031644: regulation of neurological system process	GO:0031497: chromatin assembly	GO:0007600: sensory perception
GO:0045087: innate immune response		GO:0050890: cognition	GO:0006281: DNA repair	GO:0006816: calcium ion transport
GO:0006955: immune response		GO:0035272: exocrine system development	GO:0065004: protein-DNA complex assembly	GO:0007568: aging
GO:0008063: Toll signaling pathway		GO:0022008: neurogenesis	GO:0006259: DNA metabolic process	
GO:0008219: cell death			GO:0006325: chromatin organization	
GO:0035070: salivary gland histolysis			GO:0032933: SREBP-mediated signaling pathway	
GO:0048102: autophagic cell			GO:0008593: regulation of Notch	

death GO:0016271: tissue death GO:0007559: histolysis GO:0012501: programmed cell death GO:0006865: amino acid transport GO:0006508: proteolysis GO:0006582: melanin metabolic process GO:0006570: tyrosine metabolic process			signaling pathway GO:0010627: regulation of protein kinase cascade GO:0045165: cell fate commitment GO:0008356: asymmetric cell division GO:0007164: establishment of tissue polarity GO:0051605: protein maturation by peptide bond cleavage GO:0007218: neuropeptide signaling pathway GO:0006836: neurotransmitter transport GO:0001505: regulation of neurotransmitter levels GO:0007269: neurotransmitter secretion GO:0007090: regulation of S phase of mitotic cell cycle GO:0007346: regulation of mitotic cell cycle GO:0045132: meiotic chromosome segregation	

Acknowledgements

We thank the Bloomington *Drosophila* Stock Center (USA) for providing fly stocks, Developmental Studies Hybridoma Bank (DSHB, Iowa, USA) for the anti-Broad-Core and Dr. P. Leopold (France) for the anti-Dilp8. We thank the DBT-BHU Interdisciplinary School of Life Sciences for the Microarray and real time PCR facilities.

Competing interests

Authors declare no conflicting interests

Author contributions

MR and SCL planned experiments, analyzed results and wrote the manuscript. MR carried out the experimental work and collected data.

Funding

This work was supported by a research grant (no. BT/PR6150/COE/34/20/2013) to SCL by the Department of Biotechnology, Ministry of Science and Technology, Govt. of India, New Delhi. SCL was also supported by the Raja Ramanna Fellowship of the Department of Atomic Energy, Govt. of India, Mumbai and is currently supported as Senior Scientist by the Indian National Science Academy (New Delhi). MR was supported by the Council of Scientific & Industrial Research, New Delhi through a senior research fellowship.

Data availability

The microarray data have been deposited at GEO repository (http://www.ncbi.nlm.nih.gov/geo/query/acc.cgi?acc=GSE80703).